

von **KARMAN INSTITUTE**
FOR FLUID DYNAMICS

TECHNICAL NOTE 81

THE DEVELOPMENT OF A LASER-DOPPLER VELOCITY
METER FOR THE MEASUREMENT OF SOLID PARTICLE
VELOCITY IN A TWO - PHASE FLOW

by

R.H. BARKER, Jr

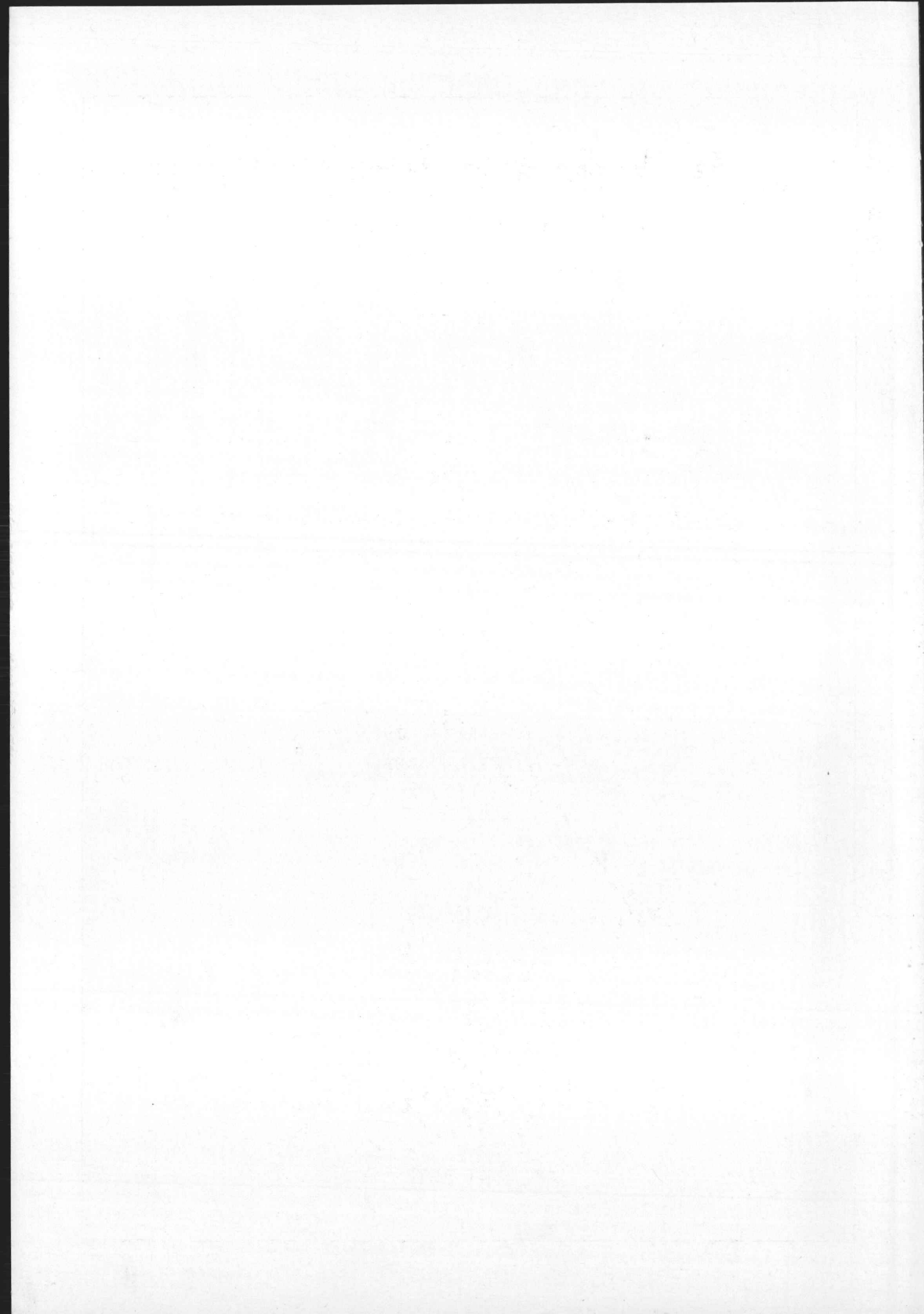
M.L. RIETHMULLER

J.J. GINOUX



RHODE - SAINT - GENESE, BELGIUM

OCTOBER 1972



VON KARMAN INSTITUTE FOR FLUID DYNAMICS

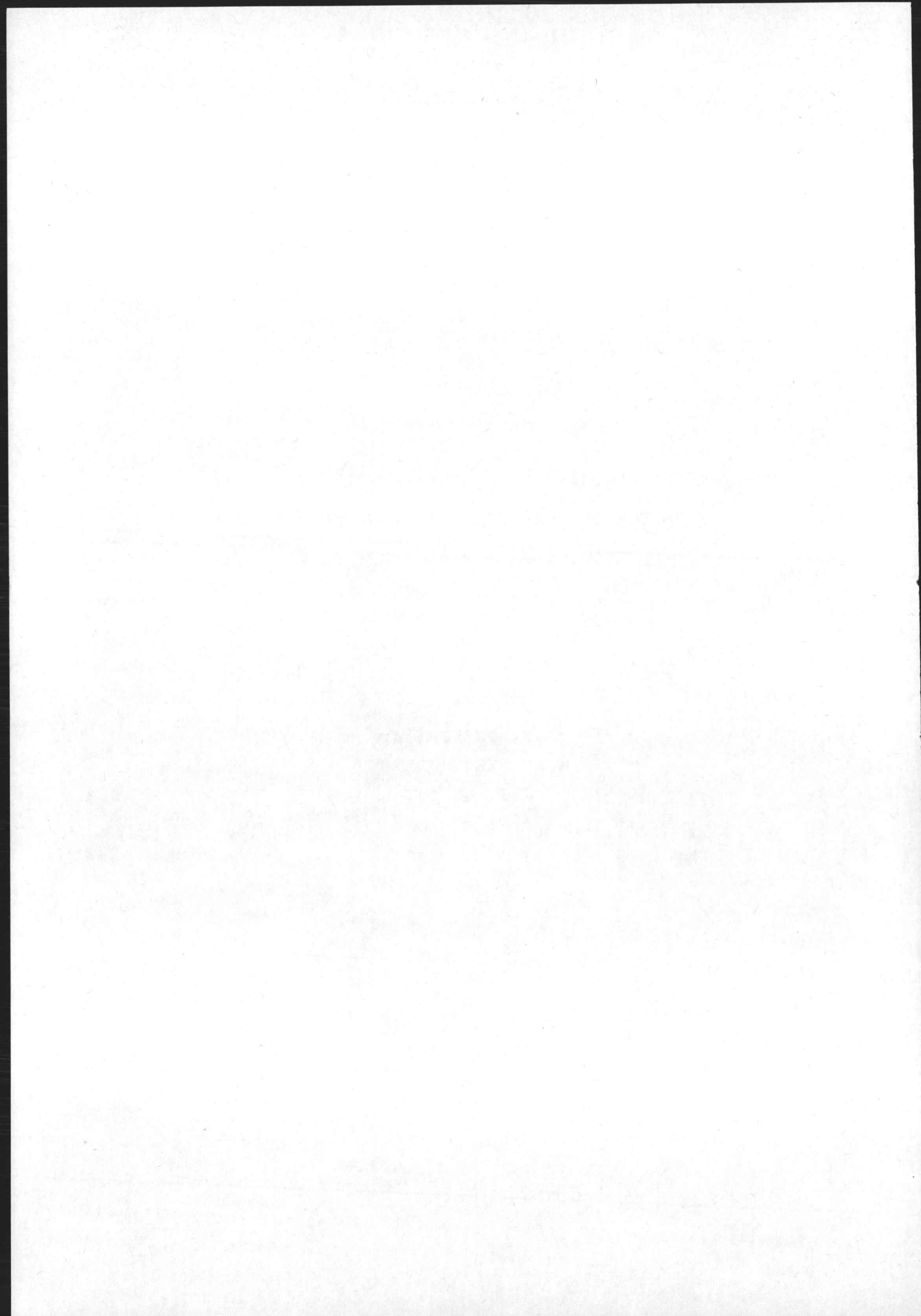
TECHNICAL NOTE 81

THE DEVELOPMENT OF A LASER-DOPPLER VELOCITY
METER FOR THE MEASUREMENT OF SOLID PARTICLE
VELOCITY IN A TWO - PHASE FLOW

by

R.H. BARKER, Jr
M.L. RIETHMULLER
J.J. GINOUX

OCTOBER 1972



ABSTRACT

A laser-doppler "fringe" velocity meter was developed with the use of simple optical equipment and low laser power (less than 1 milliwatt), for the measurement of the velocity of solid particles (diameter up to 500 microns) in a two-phase flow. The potential for a higher signal-to-noise ratio and the ease of alignment made the fringe technique more appealing than other laser-doppler methods for the present application of velocity measurements between zero and 20 meters per second.

A rotating simulation wheel was used during the development which used small wires of 100 to 500 microns in diameter to provide a most satisfactory representation of the actual particle and fringe pattern interaction. The present system gave doppler signals of extremely good quality with accurate velocity readings. The results demonstrated the successful use of a fringe laser-doppler system to measure the velocity of particles of a size much greater than the average fringe spacing. For a fringe separation of about 35 microns, successful velocity measurements of 100 and 500 micron spherical glass particles in a gas nozzle flow were made. The present system may easily be extended to a much larger velocity range by utilizing the full power of the 1 milliwatt He-Ne laser.

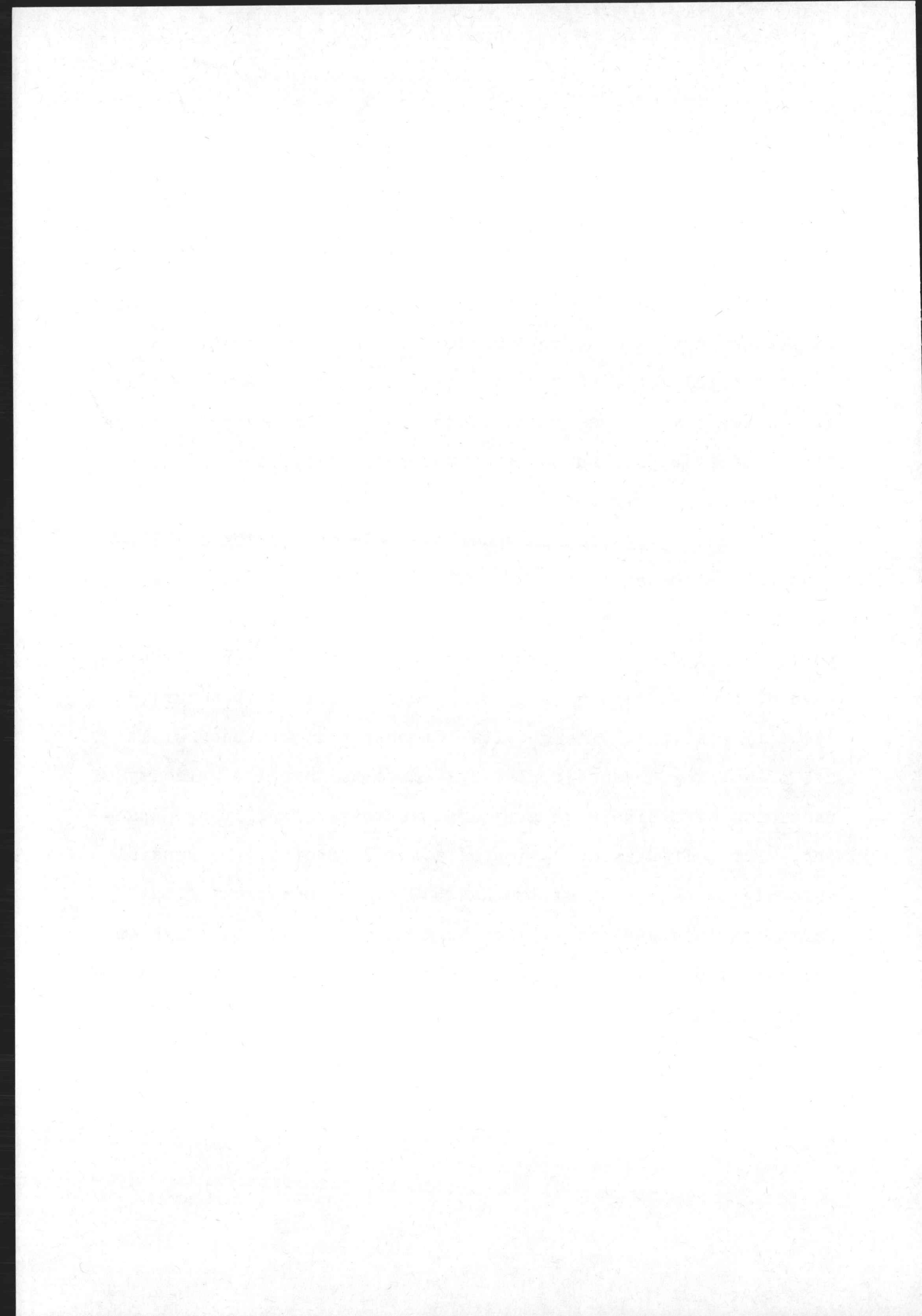


TABLE OF CONTENTS

	Page
Acknowledgement	ii
List of Figures	iii
List of Symbols	v
Introduction	1
Operating Principles	3
Experimental Procedure	14
Results	20
Recommendations	25
Conclusions	26
References	27
Figures	28
Appendix 1 Integrated Optical Unit	52
Appendix 2 Velocity Meter Apparatus	54

Acknowledgement

The assistance of Dr Trolinger of ARO, Inc. in the development of an operational laser-doppler velocity meter at V.K.I. is highly appreciated.

LIST OF FIGURES

	Page
Figure 1 Doppler Shift Geometry	28
Figure 2 Laser Focusing	28
Figure 3 Fringe System	29
Figure 4 Fringe Velocity Signal	30
Figure 5 Two Beam Illumination Doppler Shift	30
Figure 6 Fringe Probe Volume	31
Figure 7 Reference Beam Optics	32
Figure 8 Reference Beam Cross Over Region	33
Figure 9 Solid Collection Angles	34
Figure 10 Gas Particles Facility -Pl-	35
Figure 11 Laser Doppler Test Set Up	36
Figure 12 Simulation Wheel	38
Figure 13 Fringe Pattern	39
Figure 14 Signal Visibility	40
Figure 15 Wire Reflection	41
Figure 16 Signal, Particle on Simulation Wheel	42
Figure 17 Signal, Wire on Simulation Wheel, $D_f = 140 \mu$	43
Figure 18 Signal, 500 micron Particle, $D_f = 140 \mu$	43
Figure 19 Signal, Wire on Simulation Wheel, No Filter, $D_f = 106 \mu$	44 44
Figure 20 Signal, Wire on Simulation Wheel, High/Low Pass Filter, $D_f = 106 \mu$	44
Figure 21 Signal, Wire on Simulation Wheel, Low Pass Filter, $D_f = 28 \mu$	45
Figure 22 Signal, Wire on Simulation Wheel, No Filter, $D_f = 34.2 \mu$, $V = 4.78 \text{ m/s}$	46

Figure 23	Signal, Wire on Simulation Wheel, No Filter, $D_f = 34.2\mu$, $V = 12.35$ m/s	46
Figure 24	Signal, 100 micron Particle, Low Pass Filter, $D_f = 30.4$ microns	47
Figure 25	Signal, 500 micron Particle, No Filter, $D_f = 34.6\mu$, $V = 3.65$ m/s	48
Figure 26	Signal, 500 micron Particle, No Filter, $D_f = 34.6\mu$, $V = 6.95$ m/s	48
Figure 27	Particle and Gas Velocity	49
Figure 28	Nozzle Velocity Distribution	50
Figure 29	Nozzle Velocity Measurement	51

LIST OF SYMBOLS

- a - wire radius
 - b - laser beam radius
 - b_0 - focused laser beam radius
 - c - speed of light
 - d - distance
 - e - 2.718...
 - e - unit vector
 - f - frequency
 - f' - focal length
 - h - Planck's constant
 - i - differential power
 - l - length
 - t - time
 - x - distance
-
- A - area of photocathode
 - D - distance
 - I - A/C intensity, illuminating beam
 - I' - signal visibility
 - N - number of fringes
 - P - laser power, geometric focus
 - R - reference beam
 - S - scattered light
 - V - velocity
-
- η - quantum efficiency
 - θ - angle

- λ - wavelength
- μ - micron
- Δ - increment
- Ω - solid angle

Subscripts

- d - doppler
- f - fringe
- i - illuminating
- s - scattered

- B - background
- R - reference
- S - scattered

- o - source
- 1 - first
- 2 - second
- ⊥ - orthogonal

INTRODUCTION

The purpose of the experimental research performed during the course of this project was to measure the velocity of the solid particles in a two-phase gas-solid nozzle flow. Initial review of the literature revealed optical methods to be the most advantageous in the present application due to their inherent ability of not disturbing the flow and the difficulty of using conventional velocity measurements for the solid phase of the fluid. Among the optical techniques available were high speed photography to determine the particle trace during a known exposure time; multiple spark photography to evaluate the distance between particle positions knowing the time interval; and dual beam counting techniques to measure the time lapse between the particle passage of two parallel light beams. The application of recently developed laser-doppler velocity instruments proved to be of particular interest and provided the criteria for successful velocity measurements.

During the course of the past years laser anemometers have been developed for several aerodynamic applications, such as the measurement of velocity from 10^{-4} cm/sec to several thousand meters per second, density, temperature, and turbulence.(1, 2,3,4,5) The general consensus of authors who have had experience developing laser velocity meters is that the most efficient and economical systems are those designed for a particular application (ie, velocity, particle size, particle density, flow geometry, etc.). The major applications have been for the measurement of fluid dynamic properties by seeding the flow with submicron size particles so as not to disturb the flow

properties. Most applications required the measurement of the gaseous or liquid phase properties and did not uniquely supply information on the solid phase of the fluid. For those applications where a solid phase measurement was of interest, the solid particles were usually of the micron or submicron size.

The objective of this report is to summarize the work which has been completed in an attempt to develop an optical measurement technique which is suitable for the measurement of the velocity of large particles (500 microns) in a two-phase gas-solid nozzle flow.

OPERATING PRINCIPLES

The theoretical discussion of the measurement techniques considered includes the operating principle and comparison of the fringe and reference beam laser-doppler systems.

Doppler Frequency Shift

Utilizing a monochromatic light source of frequency f_0 , and wavelength λ_0 , to illuminate a particle moving at a velocity \bar{V} , the relative speed between the particle and the illuminating wavefront of propagation direction \bar{e}_i , is:

$$\lambda_0 f' = f_0 \lambda_0 - \bar{V} \cdot \bar{e}_i \quad (1)$$

where $c = f_0 \lambda_0$, is the speed of light. (See Fig. 1) The particle scatters light with a frequency:

$$f' = f_0 - \frac{\bar{V} \cdot \bar{e}_i}{\lambda_0} \quad (2)$$

A stationary observer views these scattered waves in the direction \bar{e}_s , at a frequency:

$$f_s = f' + \frac{\bar{V} \cdot \bar{e}_s}{\lambda_s} \quad (3)$$

or using equation 2,

$$f_s = f_0 + \bar{V} \cdot \left(\frac{\bar{e}_s}{\lambda_s} - \frac{\bar{e}_i}{\lambda_0} \right) \quad (4)$$

Now, since $\lambda_0 = \lambda_s$:

$$f_s = f_0 + \frac{\bar{V}}{\lambda_0} (\bar{e}_s - \bar{e}_i) \quad (5)$$

and the doppler shift is:

$$f_d = f_s - f_o = \frac{\bar{V}}{\lambda_o} (\tilde{e}_s - \tilde{e}_i) \quad (6)$$

The net change (doppler shift) in frequency observed by the viewer is due to the speed of the particle and the orientation of the particle trajectory with the illuminating \tilde{e}_i , and scattered \tilde{e}_s , light directions.

If scattered light is superimposed upon unscattered light from the same source, the signal output of a photomultiplier observing this superposition (or optical beating) will exhibit a doppler frequency tone (6). If the two waves are critically aligned, the signal will provide frequency information from the photomultiplier output from which the velocity of the moving particles can be measured. The basic principle of laser-doppler velocity measurement is the evaluation of this frequency shown in equation 6 by analysis of the signal recorded by the photomultiplier and displayed on an oscilloscope or other electronic signal analysis equipment (ie, spectrum analyzer, frequency counter, frequency tracker). (6,7)

Laser Source

Before continuing the development of the two primary laser-doppler techniques, it is perhaps appropriate to discuss the unique laser characteristics which make it most suitable for frequency shift measurement. The laser light produces a highly monochromatic light with good temporal coherence, or frequency stability. These laser characteristics allow high illumination by focusing and establish long coherence lengths over which the phase coherence is maintained. The coherence length may be

represented by:

$$l_{\text{coh}} \approx \frac{c}{\Delta f} \approx \frac{\lambda^2}{\Delta \lambda} \quad (7)$$

Since the laser is of good temporal coherence, the wavelength difference $\Delta \lambda$, is extremely small, making l_{coh} very large. (7)

Focusing of the laser beam provides a high illumination on the particles whose velocity is of interest thereby increasing the intensity of the scattered doppler shifted light. The finite extent to which a laser beam can be focused is shown in Fig. 2. This leads to a very small scattering volume which tends to eliminate much of the flow region and provide reasonable assurance that a single particle is being observed and its velocity measured. There remains, however, the limitation of measuring a single velocity component.

With these few basic laser characteristics one can now consider the theoretical development of the fringe and reference beam laser-doppler velocity measurement techniques.

Fringe Technique

The basic principles of the fringe technique can be described by calculating the doppler shifts from two equal intensity laser beams focused to a common point in space. Scattered radiation is reflected from a common particle in a common direction from the two beams, and yields a doppler shifted frequency which is independent of the viewing direction and of a constant value for a given particle velocity. Another development describing the formation of an interference or "fringe" pattern by the two converging beams allows an easier understanding of the operating characteristics and design principles of

this method. Both developments will be summarized to better understand how the fringe technique compares to both the reference beam laser-doppler technique and the dual beam counting methods.

A schematic diagram of the fringe system is shown in Fig. 3. Two parallel beams are focused to a common point in the flow, maintaining their spacial and temporal coherence properties. The focused beams form long, narrow, pencil shaped beams with a Gaussian intensity distribution and essentially planar wavefronts. The two radiations interfere to form a series of light and dark fringes. Any two of these fringes are separated by the distance:

$$D_f = \frac{\lambda}{2 \sin \theta/2} \quad (8)$$

The photomultiplier detects the velocity of a moving particle across the fringe pattern by detecting the variations of light intensity between the light and dark fringes and displaying an electrical current in the fashion shown in Fig. 4, with a DC signal showing the particle passage through the focal volume and an AC modulation proportional to the rate of the fringe passage. The frequency of the AC or doppler signal is:

$$f_d = \frac{2 \sin \theta/2}{\lambda} V_{\perp} \quad (9)$$

which is equivalent to the doppler shifted radiation from a common particle located at the intersection of the two beams.

As mentioned above, the doppler frequency can be explained by considering the heterodyning of two radiations scattered from a common particle illuminated from two different directions as shown in Fig. 5. The optical alignment is identical to that of

Fig. 3. The two illuminating beams are travelling in directions \tilde{e}_{i1} and \tilde{e}_{i2} , respectively, and are being viewed from the direction indicated by \tilde{e}_s . Light scattered from beam 1 is of frequency:

$$f_{s1} = f_0 + \frac{\bar{V}}{\lambda} \cdot (\tilde{e}_s - \tilde{e}_{i1}) \quad (10)$$

and light scattered from beam 2 is of frequency:

$$f_{s2} = f_0 + \frac{\bar{V}}{\lambda} \cdot (\tilde{e}_s - \tilde{e}_{i2}) \quad (11)$$

When these two radiations intercept a photodetector, they generate a doppler signal of frequency:

$$f_d = \frac{\bar{V}}{\lambda} \cdot (\tilde{e}_{i2} - \tilde{e}_{i1}) = \frac{2 \sin \theta/2}{\lambda} \bar{V} \cdot \tilde{e}_\perp \quad (12)$$

where \tilde{e}_\perp is orthogonal to $(\tilde{e}_{i1} + \tilde{e}_{i2})$. It can easily be seen that this frequency is identical to that of equation 9, where the velocity component measured is orthogonal to the mean illuminating direction and to the fringe pattern established by the interference of the two beams.

The detected frequency, f_d , is independent of the viewing direction; thus the signal strength can be increased by increasing the solid collection angle of the viewing optics without altering the observed frequency. As will be shown later, the solid collection angle for reference beam techniques must be limited to prevent frequency broadening effects. The use of a rather large viewing lens for collecting the scattered light does introduce the requirement for an aperture at the photodetector to avoid collecting unwanted signals. The aperture size must be matched to the size of the image of the focal volume

that is established at the photodetector to avoid the collection and measurement of stray signals which introduce noise contributions to the laser doppler signal. (4,5,6)

The probe volume characteristics are shown in Fig. 6 and are represented by the dimensional relationships: (4)

$$\text{beam width: } 2b_0 = \frac{4}{\pi} \frac{f'}{2b} \lambda \quad (13)$$

$$\Delta x(1/e^2) = 2b_0$$

$$\Delta y(1/e^2) = 2b_0 / \cos \theta/2 \quad (14)$$

$$\Delta z(1/e^2) = 2b_0 / \sin \theta/2$$

The number of fringes can be computed from:

$$N(1/e^2) = \frac{2b_0}{\lambda} \frac{2 \tan \theta/2}{1} \quad (15)$$

$$\text{or } N(1/e^2) = \frac{4}{\pi} \frac{D}{2b} \quad (16)$$

where N = number of fringes

$D = 2f' \tan \theta/2$ parallel beam separation

$2b =$ unfocused beam diameter

$2b_0 =$ focused beam diameter

Increasing the number of fringes will increase the accuracy of the velocity measurements by providing a greater number of signal cycles from which the average frequency value may be taken. As the number of fringes increases for a fixed velocity, or as the velocity increases for a fixed number of fringes, a smaller number of photons are scattered from each fringe. This can lead to the requirement for more laser power and more sensitive light detecting equipment. (7)

The fringe system is similar in nature to the dual beam counting methods, since in principle one measures the time lapse of a particle passing between two parallel fringes at a known

distance. It is also analogous to the reference beam technique, since the velocity measurement can be obtained by considering the optical beating of the scattered radiation from two illuminating beams. (8)

Reference Beam Technique

The schematic diagram for a reference beam geometry laser-doppler system is shown in Fig. 7. The optical system focuses each laser beam to a common point in the flow region. The reference beam that intersects the photodetector directly is of low power relative to the second beam which reflects scattered light as a particle passes the focal region. (This is in contrast to the fringe system where two beams of equal intensity intersect to provide the most distinct fringe pattern and signals.)

The light scattered from the plane waves of propagation direction \vec{e}_i by moving scatterers in the focal region is doppler shifted by the amount:

$$f_d = \frac{V}{\lambda_0} \cdot (\vec{e}_s - \vec{e}_i) = \frac{2}{\lambda} \sin \theta/2 \quad V \cdot \vec{e}_1 \quad (17)$$

with the velocity component being measured normal to the plane of the beam intersection.

The reference beam of low intensity is incident upon the photodetector essentially unscattered and therefore is not frequency shifted. Light scattered from the particle by the high power illuminating beam reflected along the vector \vec{e}_s coincident with the reference beam direction. These two radiation sources interfere at the photodetector and generate a current of frequency f_d .

The probe measurement volume is defined as the region in space at the beam intersection where the relative harmonic doppler signal current amplitude is at least $1/e^2$ of that maximum possible current amplitude which occurs when a particle passes the point P shown in Fig. 8. This $1/e^2$ probe volume is contained within the $1/e^2$ intensity contours of the I and R beams.

The doppler current generated by a single scatterer is not of a unique frequency, f_d , but is slightly dispersed about a mean frequency, \bar{f}_d . This frequency dispersion is caused by the finite angle $\Delta\theta$ (see Fig. 9) of the scattered radiation which is superimposed upon and aligned with the reference beam at the photodetector surface. $\Delta\theta$ is the angle of the $1/e^2$ intensity contour of the converging reference beam. This angle is essentially constant at points remote from the geometric focus, P. The net frequency dispersion, Δf_d , due to a finite $\Delta\theta$ is determined to be:

$$\begin{aligned} \Delta f_d / f_d &= \frac{\Delta\theta}{2} \cot \bar{\theta} / 2 \\ &\approx \frac{\Delta\theta}{\bar{\theta}} \text{ (small } \bar{\theta} \text{)} \end{aligned} \quad (18)$$

For small front scattering (small $\bar{\theta}$), the angle $\Delta\theta$ is made much smaller than $\bar{\theta}$ to minimize signal frequency dispersion and provide an accurate doppler signal. A value of 0.05 for $(\frac{\Delta f_d}{\bar{f}_d} - \frac{\Delta\theta}{\bar{\theta}})$ will provide a velocity measurement with an accuracy of about one percent. The small value of $\Delta\theta$ limits the signal-to-noise ratio as the effective solid collection angle of the scattered radiation, $\Delta\Omega = \Delta\theta^2$, is restricted. (6)

Aperture requirements arise for the reference beam technique to insure that the photodetector only views a small $\Delta\theta$ and no background noise or spurious reflections from other particles

in the flow. Alignment is more complicated than the fringe method, since one does not have the advantage of the collecting lens to project an image of the focal volume to the aperture; and the requirement for small $\bar{\theta}$ makes positioning of the filter on the reference beam more difficult due to the narrow separation between the two beams prior to the lens. Additionally, particles not crossing the probe volume exactly through the point P as shown in Fig. 8, will exhibit some frequency broadening in their doppler signals due to the inherent misalignment of the reference and scattered beams which propagates over the distance to the photodetector.

Signal-To-Noise Ratio Problems

To more easily understand the signal-to-noise problems encountered in the use of laser-doppler systems, one must consider the general signal-to-noise ratio applied to both the fringe and reference beam techniques. Following the development of Reference 6, the expression for signal-to-noise ratio may be written:

$$\text{SNR} = \frac{\eta A}{hf_1 \Delta f} \left(\frac{S_1 S_2}{S_1 + S_2 + S_B} \right) \quad (19)$$

where η is the quantum efficiency of the photodetector

A is the radiated area of the photodetector

h is Planck's constant

f_1 is the laser beam frequency

Δf is the bandwidth of the photodetector

$S_1 S_2$ the intensity of the beams

S_B the background light intensity

For the reference beam technique, equation 19 becomes:

$$\text{SNR} = \frac{\eta A S_S S_R}{h f_1 \Delta f (S_S + S_R + S_B)} \quad (20)$$

where S_R & S_S are the reference and scattered light beam intensities, and AS_S is the aligned scatter power within the $1/e^2$ intensity region of the reference beam as it diverges from the scatter point. Since:

$$\frac{S_R}{S_S + S_R + S_B} \approx 1 \quad (21)$$

AS_S is related to the solid collection angle of the reference beam by:

$$AS_S \approx i_s(\theta) \Delta\theta^2 \quad (22)$$

where $i_s(\theta)$ is the differential scattered power. $\Delta\theta^2$ must be small to limit frequency broadening effects.

For the fringe system the two beams are of equal intensity, $S_1 = S_2$, and equation 19 becomes:

$$\begin{aligned} \text{SNR} &= \frac{A}{h f_1 \Delta f} \frac{S_1^2}{2S_1 + S_B} \quad S_B \ll 1 \\ &\approx \frac{\eta i_s(\theta) \Delta\theta_s^2}{2h f_1 \Delta f} \end{aligned} \quad (23)$$

where AS_1 is the aligned scatter power at the photocathode and $\Delta\theta_s^2$ is the solid collection angle of the scattered radiation. Since $\Delta\theta_s^2$ is not limited by frequency broadening as in the reference beam method, the signal-to-noise ratio can be increased by using a larger diameter collecting lens.

By referring again to equation 19, one can see that for a given photodetector, the only mechanism for further increasing

the signal-to-noise ratio is by using a higher power laser to increase S_1 & S_2 since a direct increase in the photocathode area is not possible because of aperture requirements.

EXPERIMENTAL PROCEDURE

The development of a laser-doppler technique for the measurement of solid particles was directed towards utilization in the VKI two-phase, gas-solid flow facility, Pl, where velocities up to about 20 meters per second are presently experienced. The application of the device for higher velocities was left for future development. A picture of the flow facility is shown in Fig.10,(see ref11) and one can see the location of the test section where the velocity measurements were made. The moving gas flowed through the horizontal pipe at a constant velocity, and the solid particles were injected into the flow from the reservoir by use of a valve to regulate the loading ratio. A mixer could be employed to inject the particles (spherical glass beads of 100 to 500 microns in diameter) into the gas with an initial velocity parallel to the gas flow. The particles were then accelerated by the gas and the two-phase flow exited a nozzle of circular cross section into the test section. The particles could subsequently be collected and reloaded into the facility as shown.

Several optical arrangements were investigated so as to duplicate the measurement techniques previously discussed. In order to avoid the undesirable situation of testing in the actual flow facility, an alternate means of simulating the flow was devised. A circular plexiglass disc was mounted on a motor axis. Solid particles of the same type as used in the flow facility (diameter = 500 microns) were randomly affixed to the surface of the disc with a transparent spray. This simulation was used for the laser-doppler experiments for the measurement of

the tangential component of the particle velocity. An advantage of the simulation device was that it provided an excellent means of checking the accuracy of the velocity meter before actual flow testing. One simply compared the measured velocity values to those computed knowing the disc revolution rate and the position of the particle. Once developed, the laser-doppler device had the advantage of not requiring any calibration before use as with conventional velocity measurement devices.

With the aid of Dr. Trolinger of ARO, Inc. a fringe method laser-doppler velocity meter was developed with a set of very crude optics. The fringe method was utilized because of the potentially better signal-to-noise ratio and ease of implementation with simple optical equipment. The optical system is shown in Fig. 11, and used a very thin flat plate window glass (1.15 mm) to reflect a small portion of the full laser power in two parallel beams from its surfaces. The major portion of the 1 milliwatt He-Ne laser light was simply transmitted through the glass and not used for velocity measurements. The two parallel beams were focused by a converging lens ($f' = 165$ mm) to a common point, and subsequently formed a fringe or interference pattern. The pattern could be analyzed by observing its projection onto a viewing screen with the use of a microscope lens. By measurement of the fringe spacing and knowledge of the magnifying power of the microscope, one had an excellent means of comparing it to the calculated values from equation 8.

The viewing optics consisted of a collecting lens ($f' = 100$ mm) for the scattered light which projected an image of the focal volume (and fringe pattern) to an aperture 0.4 mm wide mounted in front of the photocathode at the face of the photo-

multiplier, which recorded the laser-doppler frequency signal. The photomultiplier was an EMI model 9558 with an S-20 cathode surface which had a spectral response sufficient to measure the light of the laser at 6328 angstroms. A high negative potential of 1400 volts was supplied to the photomultiplier and then varied slightly to provide minimum noise levels depending on the room background noise levels. The aperture served the purpose of filtering stray signals, and in conjunction with the collecting lens provided an excellent means of improving the signal-to-noise ratio even in the presence of ordinary room light during the testing period.

The focusing and viewing optics were mounted on separate optical benches with three degree of freedom adjustable supports for the collecting lens and the photomultiplier, allowing fine adjustment of the optical alignment. The optical benches were supported by a heavy metal table with a wooden top to prevent vibrations from distorting the fringe pattern.

The alignment procedure of the system consisted of projecting the laser beam at the reflecting glass and having the two reflections pass through the converging lens to the measurement point. Because of the slightly skew nature of the two surfaces of the glass, it had to be rotated to a proper position to provide parallel beams. The parallel nature of the beams was observed when the projection of the focal volume by the microscope lens indicated the beams were aligned at the cross over region and the fringe pattern was the most distinct attainable. Having obtained a good quality fringe pattern, the collecting lens was positioned at a distance from the focal region slightly greater than its focal length thereby projecting a real, magni-

fied image to the aperture at the photomultiplier. The photomultiplier signal was then displayed on a storage oscilloscope, and the signal quality was optimized by final adjustment of the viewing optics.

The storage scope was employed in the trigger mode which allowed a signal display only when a sufficiently high amplitude of the AC doppler signal was detected. The trigger level could be adjusted and only signals above that level recorded. In this way velocity measurements could be made only of those particles which crossed the fringe pattern at its center and provided the highest amplitude and best quality signals, thereby acting as a filtering device if one wished to utilize this capability.

The use of electronic filtering devices also aided the signal processing and display procedure. Low pass filters were employed to eliminate noise and stray signals whose frequencies were above the frequency of the doppler signal. With the additional use of high pass filters, one could eliminate the DC component of the doppler signal, and have a signal which only contained the doppler frequency from which the velocity information could subsequently be processed by use of frequency counters or other electronic display equipment (6,7). This means of data processing has the potential of providing very accurate results for the velocity since one would electronically measure the signal frequency rather than visually as is done with the oscilloscope display.

During the experimental process, several different types of filters were used. A variable active filter with a 200 KHz maximum frequency capability and both low and high pass capa-

bility proved useful for the lower velocity range (ie, 35 micron fringe spacing and velocities up to 7 m/s). For increased velocity both a 500 KHz passive filter and a 40 to 430 KHz band active filter were used, providing filtering up to 17 and 15 m/s, respectively. Experience showed the active filters to provide a more accurate signal display and less distortion of the velocity data due to their more rapid response times and more sharply defined frequency limits. Additionally, one had to use care that the filtering process did not distort the true velocity values.

Initial signals obtained from the laser-doppler system used with the simulation wheel indicated a frequency shift was present, but were not of sufficient clarity to provide any velocity data. In an attempt to improve the simulation, a new disc was used which contained small wires (diameter = 100-500 microns) projecting radially outward from the circumference. This eliminated the possibility of reflection and refraction of the laser light by the disc and the spray surrounding the particles. The use of the wire as shown in Fig. 12 proved to be the most efficient means of simulating the particle and fringe pattern interaction.

A photograph of the fringe pattern is shown in Fig. 13, where the two beams crossed at an angle of 2.25 degrees forming approximately 11 fringes in the $1/e^2$ intensity area with a spacing of 32 microns. The probe volume dimensions in the Δx and Δy directions were approximately 350 microns. The number of fringes can be varied by changing the angle between the two laser beams. The easiest means of achieving this is to use an integrated optical unit as shown in Appendix 1. The present

system uses different thickness reflecting glass (1.15 & 11.25 mm) and different angles of incidence of the laser beam to vary the number and spacing of the fringes.

RESULTS

Of primary concern during the testing period of the fringe system were the pattern quality and proper matching of the fringe spacing to the particle size. The relatively simple optical equipment utilized provided excellent fringe patterns as was evidenced in Fig. 13, which were relatively insensitive to vibrations except when the system was used adjacent to a running continuous supersonic wind tunnel. Some distortion of the fringe pattern was observed which destroyed the clarity of the frequency information. In severe situations shock insulation of the optical benches may be required to prevent signal distortion. Referring to Fig. 14, one can observe the variation of signal visibility vs particle size as predicted by small particle scattering theory. The signal visibility, I' , is defined from the AC doppler signal as the ratio between the difference and the sum of the maximum and minimum intensities of the modulated signal. This reflection analysis, when compared to the experienced values of I' for a 300 micron wire simulating the particle, shows considerable disagreement. At a fringe spacing of 35 microns with the 300 micron wire, one would expect an extremely small signal visibility. Analysis of the signals experienced showed values for I' around 0.5, indicating a much smaller particle was present. Because of this phenomena and that previous fringe system developers had indicated it was not possible to apply the system to large particles (diameter > fringe spacing), an attempt was made to discover the reasons involved. (4,7) Fig. 15 shows an enlargement of the 300 micron wire in the focal volume as viewed by the photomultiplier. As can be seen, only a very small por-

tion of the wire surface area is illuminated as the fringe pattern is crossed (approximately 10%). This situation represents that of a much smaller particle of the same order of magnitude as the fringe spacing (35 microns) being observed. It was postulated that similar results would be obtained from the spherical particles in the flow facility. The results shown later will indeed prove this to be true, indicating one can measure the velocity of particles larger than the fringe spacing provided the viewing optics observe the flow from an angle sufficient to collect only the scattered light from one side of the particle. (9)

The success of the laser-doppler system which was developed is best illustrated by an analysis of the particular characteristics of several unique doppler signals that were obtained.

1) Fig. 16 illustrates the poor quality signals which were provided by the initial simulation wheel using the actual particles attached to the disc surface, and did not truly represent the interaction between the laser light and the particle due to reflections and refractions of the wheel and spray which held the particles.

2) Signal quality was improved by utilization of wires to simulate the flow and a low pass filter to eliminate stray noise contributions. Fig. 17 shows these results as obtained from the simulation wheel with the 300 micron wire; and Fig. 18 shows those for the actual flow with 500 micron particles.

3) For a rather wide fringe spacing of 106 microns, Figures 19 and 20 show a completely nonfiltered signal and one observed with the use of both a high and low pass filter. Care must be taken in application of the filter to maintain the dopp-

ler frequency, but it does provide velocity information in a format which is easy to apply to alternate display techniques such as frequency analyzers or electronic counters (6,7).

4) Using the thicker reflecting glass (11.25 mm), one can obtain a larger angle between the two beams and, hence, an increase in the number of fringes over those shown above which allows more frequency cycles over which more accurate velocity information is obtained by averaging. Fig. 21 shows a signal obtained from the 300 micron wire with a fringe spacing of 28 microns.

5) The simulation wheel was used to investigate the effect of increased velocity on the signal as shown in Figures 22 & 23, where velocities of 4.78 & 12.35 m/s are shown respectively for nonfiltered signals. It can be seen that the amplitude of the doppler signal is decreased with higher velocity, confirming the predictions of Imperial College (7).

The remainder of the results contain signals and velocity measurements which were made in the actual flow facility. A plexiglass visualization box with glass windows was placed around the exit of a 4.7 cm diameter circular nozzle to observe the flow and still maintain collection of the solid particles as the flow was exhausted into the air at atmospheric pressure. Velocity measurements were made about 1 cm from the plane of the nozzle exit with the laser beams and viewing optics utilizing the glass windows for transmittance of the light. A very slight refraction of the laser beam was observed as it entered and exited the glass windows, which did not perturb the velocity measurements.

6) Having experienced signals on the simulation wheel,

an attempt to obtain signals with smaller diameter (100 micron) particles in the flow facility proved successful as shown in Fig. 24.

7) With very precise optical alignment and aperture sizing, one can obtain quality signals without the aid of filters before display on the oscilloscope. Figures 25 & 26 show the results of measurements made in the facility with 500 micron particles at two different velocities without the aid of a filter.

8) Fig. 27 shows a comparison between the average measured particle velocity at the exit of the nozzle to theoretical predictions for the particle to gas velocity ratio using a Stokes flow drag coefficient on a spherical particle of 100 microns in diameter accelerated from zero initial velocity at its injection point in the flow. The measurements were taken at 1.6 meters from the particle injection point and the gas velocity was assumed constant over the region extending to the nozzle exit. The measurements indicated that this particular two-phase drag theory compared within 2 to 3 per cent of the actual velocities experienced.

9) The velocity of larger diameter particles (500 microns) was measured under similar conditions in a traverse of the nozzle exit as shown in Fig. 28. As can be seen, a rather uniform velocity distribution across the nozzle was experienced with a dispersion of particle velocities indicating flow irregularities. The exact location of the measurement points is somewhat uncertain due to the fact that the two separate optical benches were moved and the system realigned to make these measurements. For more precise mobility of the system, it is recommended that the

optical benches be combined into a single unit with a capability to be moved freely without necessitating realignment.

10) A final comparison was made in Fig. 29 with the 500 micron particles velocities being compared to theoretical values determined from Newtonian drag theory assuming constant drag on the spherical particles as they were accelerated by the gas flow. The values shown with and without the mixer represent the injection of the particles into the gas with and without an initial velocity component parallel to the gas flow. The measurements were made at the nozzle exit, 1.0 meter from the point of the particle injection.

RECOMMENDATIONS

1) A detailed analysis of the reflection process from large particles (diameter > fringe spacing) and their interaction with the fringe pattern should be conducted.

2) Use of the 1 milliwatt He-Ne laser full power with the integrated optical unit should be attempted to extend the present velocity range.

3) An investigation of alternate laser-doppler techniques as described in the literature and Appendix 1 should be completed to determine their applicability to the present flow situation.

4) Subsequent developers of laser-doppler systems are reminded to insure the system design is compatible with the unique requirements of the particular flow situation of interest.

CONCLUSIONS

1) Fringe laser-doppler velocity measurements can be made of solid particles much larger in size than the average fringe spacing provided the viewing optics only record the reflections of light from one side of the particle as it passes each fringe in the focal volume.

2) Very simple optical equipment and low laser power (less than 1 milliwatt) are suitable for making velocity measurements in the present application of solid particles in a two-phase flow. With increased laser power, higher velocity measurements are obtainable.

3) Small wires of the same size as the flow particles provide a most satisfactory simulation of the actual measurement process.

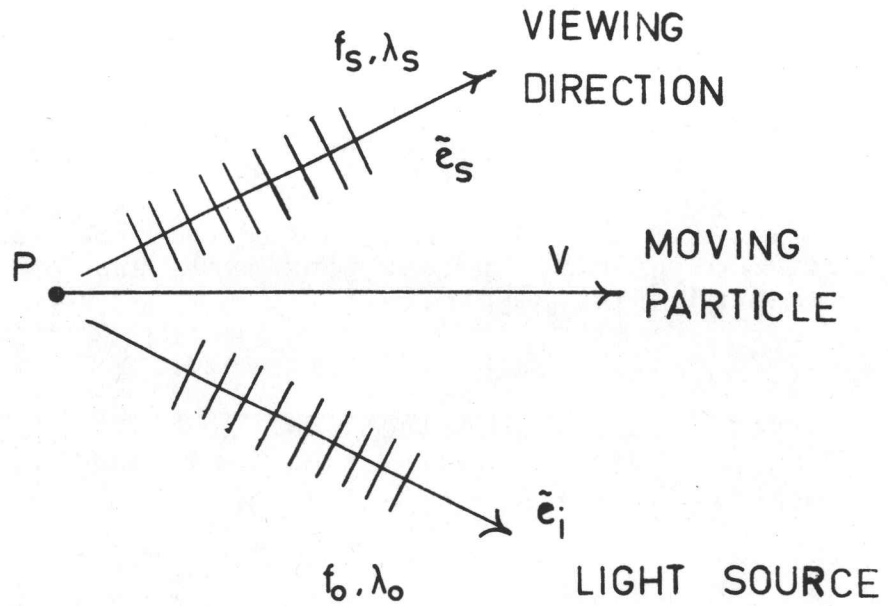
4) A greater number of fringes in the focal volume allows more accurate velocity information by providing a larger number of cycles from which an average frequency is obtained. Care must be exercised that the particle size and fringe spacing are compatible with accurate velocity measurements.

5) With the use of very precise optical alignment and viewing aperture sizing, one can obtain signals of sufficient quality to provide accurate velocity information without the aid of a filter for oscilloscope display analysis.

6) The velocity measurements can be made with no flow disturbance and offer extremely convenient means of determining solid particle velocity in a two-phase flow.

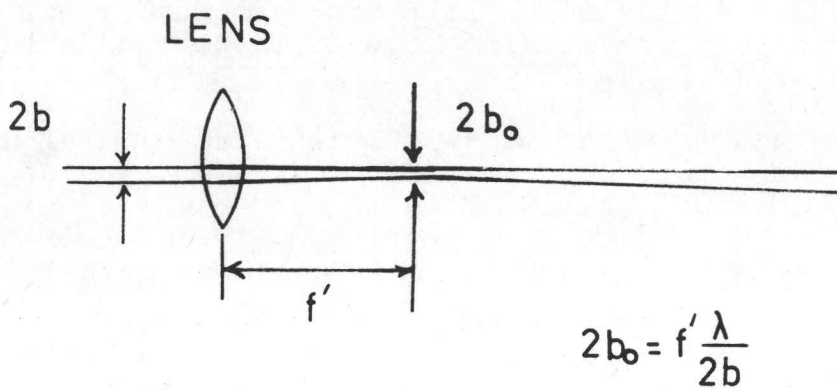
REFERENCES

- 1) James, R.N., Babcock, W.R., and Seifert, H.S., "A Laser Doppler Technique for the Measurement of Particle Velocity", AIAA J., 6, pp 100-162, Jan 1968.
- 2) Penner, S.S., "Use of Lasers for Local Measurements of Velocity Components, Species Densities, and Temperature Measurements", AIAA Paper 71-283.
- 3) NASA CR - 1199, "Laser Doppler Velocity Instrument".
- 4) Brayton, D.B., and Goethert, W.H., "A New Dual-Scatter Laser Doppler Shift Velocity Measuring Technique", ISA Transactions, Vol 10, No. 1, 1971.
- 5) Brayton, D.B., Kalb, H.T., and Crosswy, F.L., "A Two Component, Dual-Scatter Laser Doppler Velocimeter with Frequency Burst Signal Readout", Feb 29, 1972.
- 6) VKI Lecture Series 39, Vol 1, "Laser Technology in Aerodynamic Measurements", Jun 14-18, 1971.
- 7) Imperial College of Science and Technology, Lecture for a Post Experience Course, "Optical Beam Methods for Velocity Measurements", Jan 1972.
- 8) Durst, F., and Whitelaw, J.H., "Optimization of Optical Anemometers", Proc. Roy. Soc. London, A. 324, 157-181, 1971.
- 9) Farmer, W.M., "Dynamic Particle Size and Number Analysis Using a Laser Doppler Velocity Meter", to be published in Applied Optics, Jul-Aug 1972.
- 10) Durst, F., and Whitelaw, J.H., "Integrated Optical Units for Laser Anemometry", Scientific Instruments, J of Phys E, Vol 4, pp 804-808, Nov 1971.
- 11) BUCHLIN, RIETHMULLER, GINOUX, VKI Technical Note in preparation.



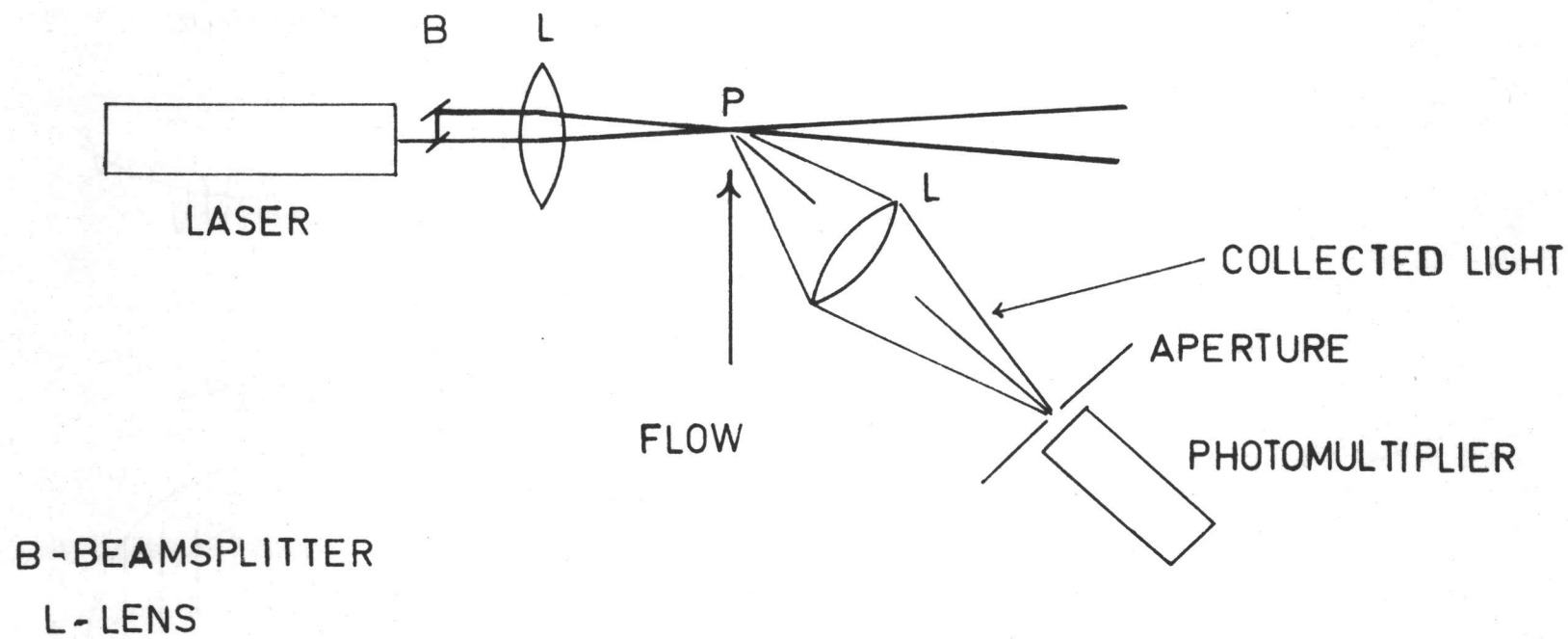
DOPPLER SHIFT GEOMETRY

Figure 1

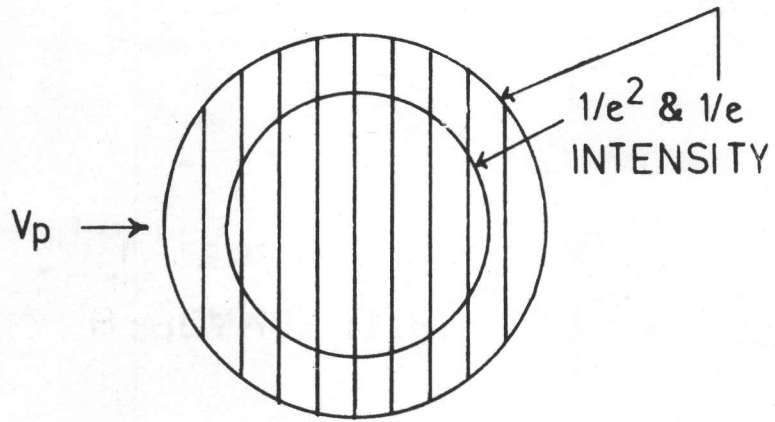


LASER FOCUSING

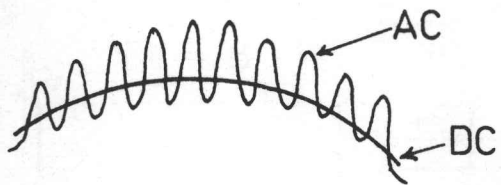
Figure 2



FRINGE SYSTEM
 Figure 3



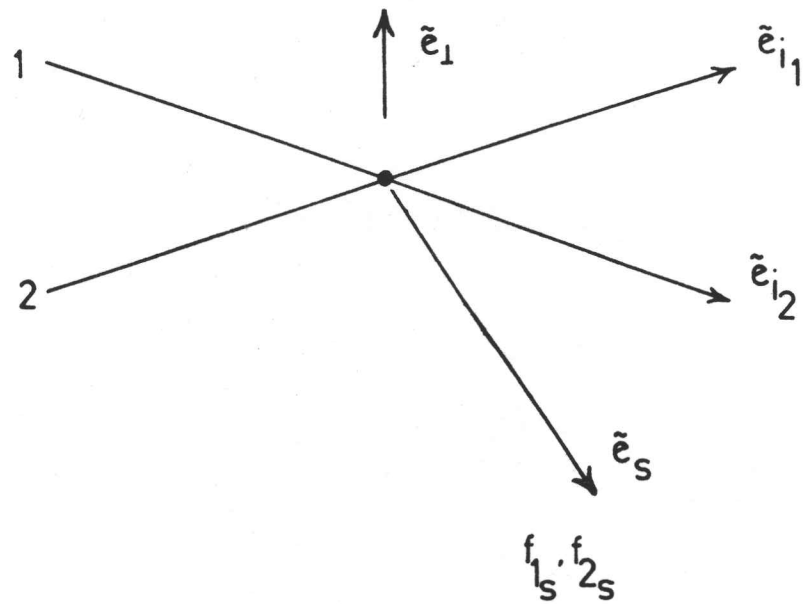
PATTERN



SIGNAL

FRINGE VELOCITY SIGNAL

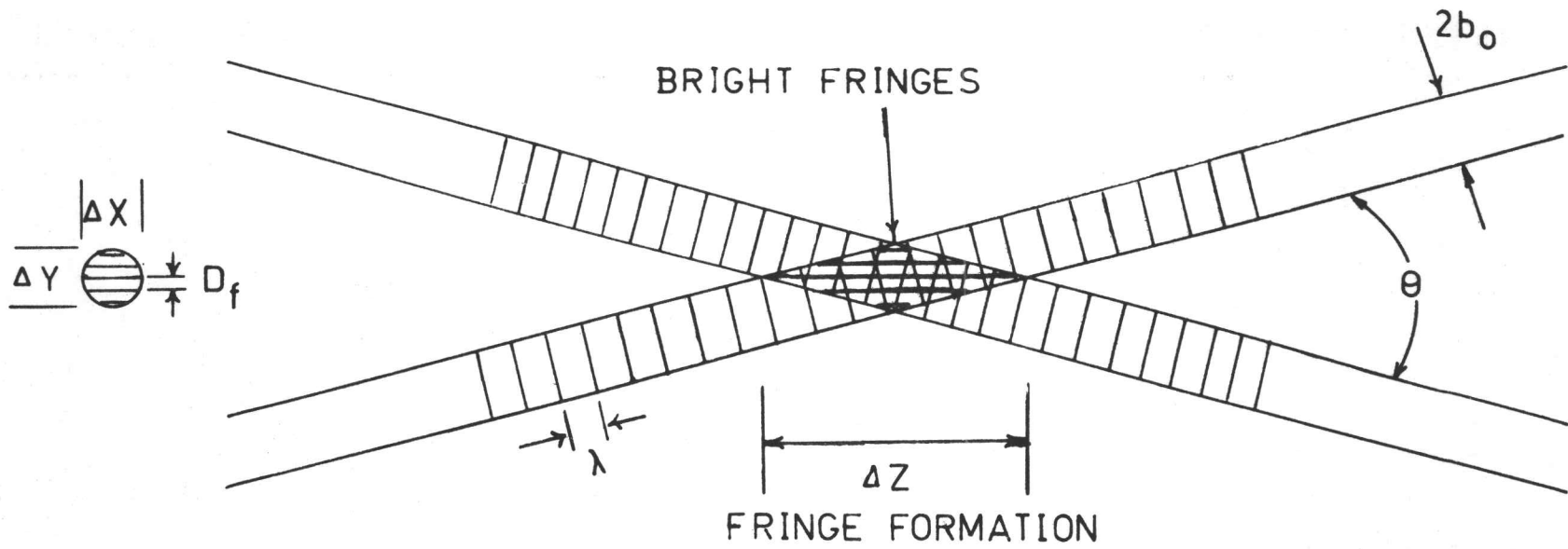
Figure 4



30

TWO BEAM ILLUMINATION
DOPPLER SHIFT

Figure 5



$$D_f = \frac{\lambda}{2 \sin \theta/2}$$

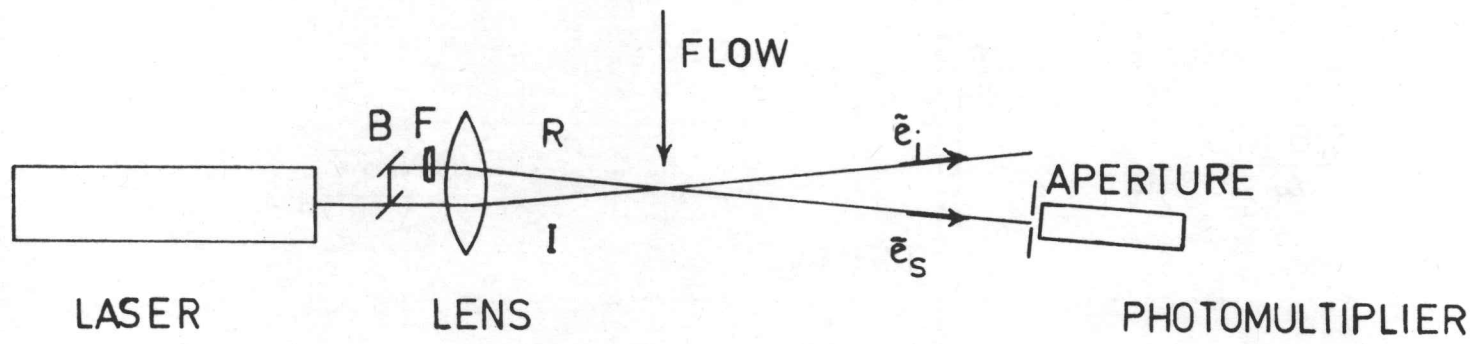
$$\Delta X = 2b_0$$

$$\Delta Y = \frac{2b_0}{\cos \theta/2}$$

$$\Delta Z = \frac{2b_0}{\sin \theta/2}$$

Figure 6

FRINGE PROBE VOLUME



B-BEAMSPLITTER

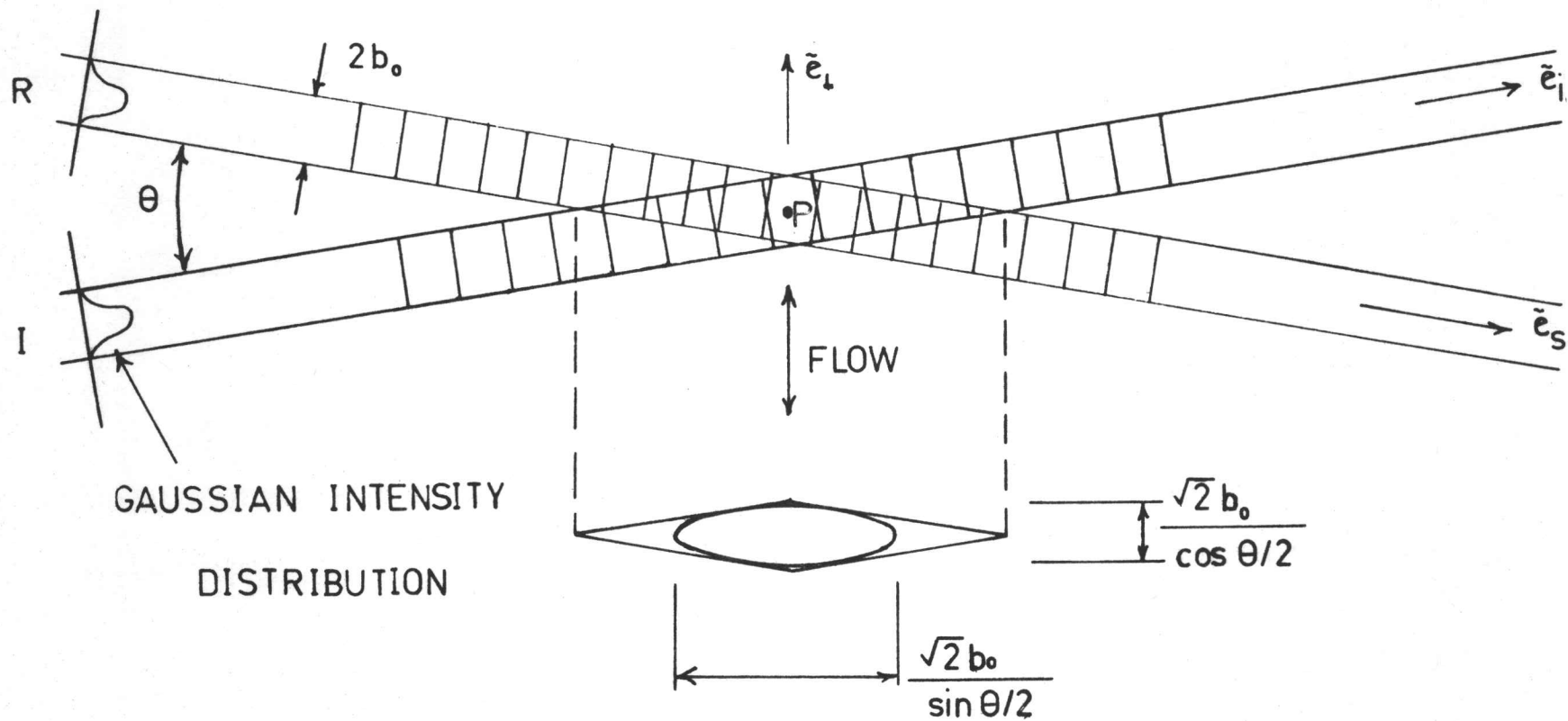
I-ILLUMINATING BEAM

F-FILTER

R-REFERENCE

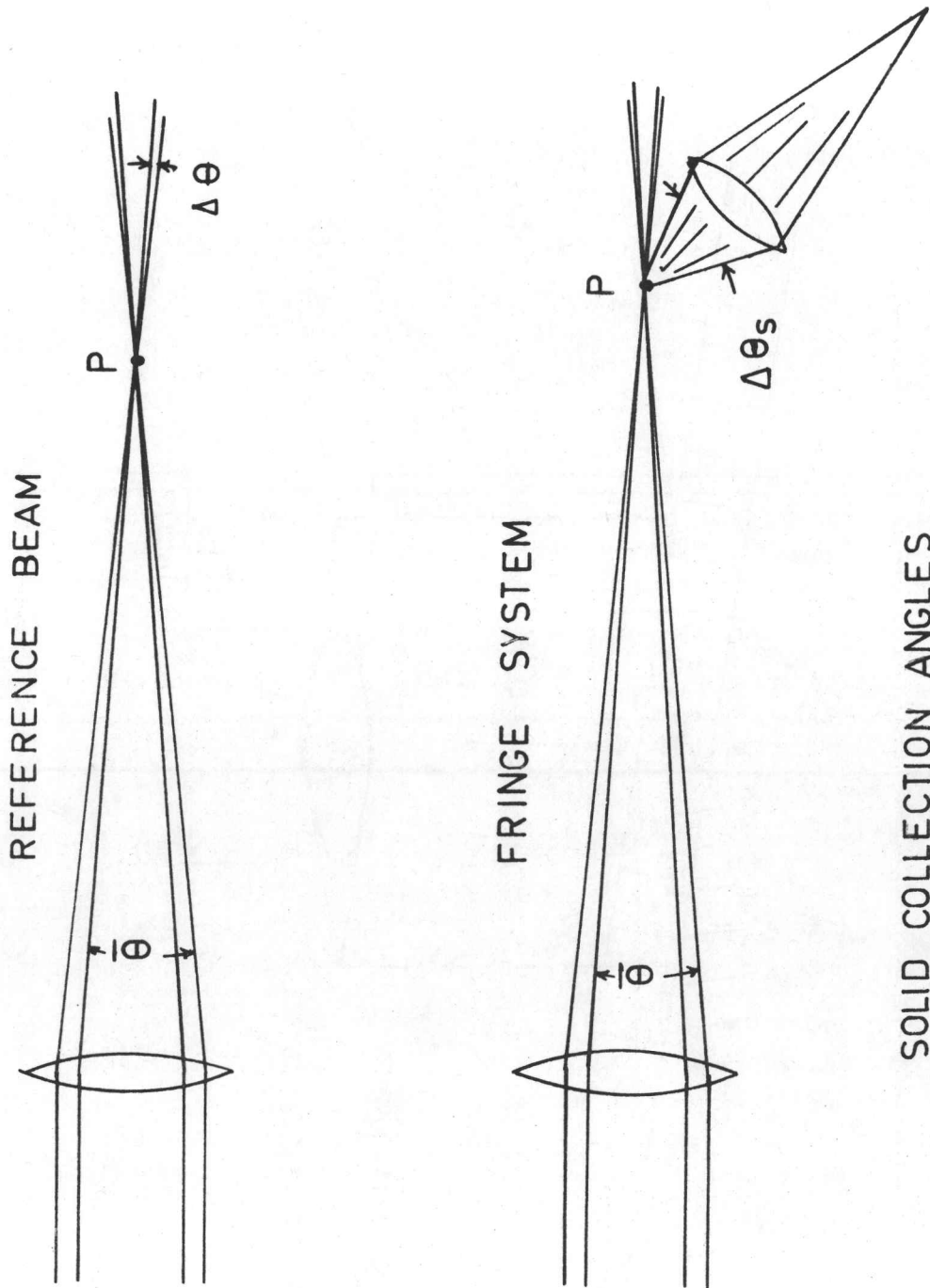
REFERENCE BEAM OPTICS

Figure 7



REFERENCE BEAM CROSS OVER REGION

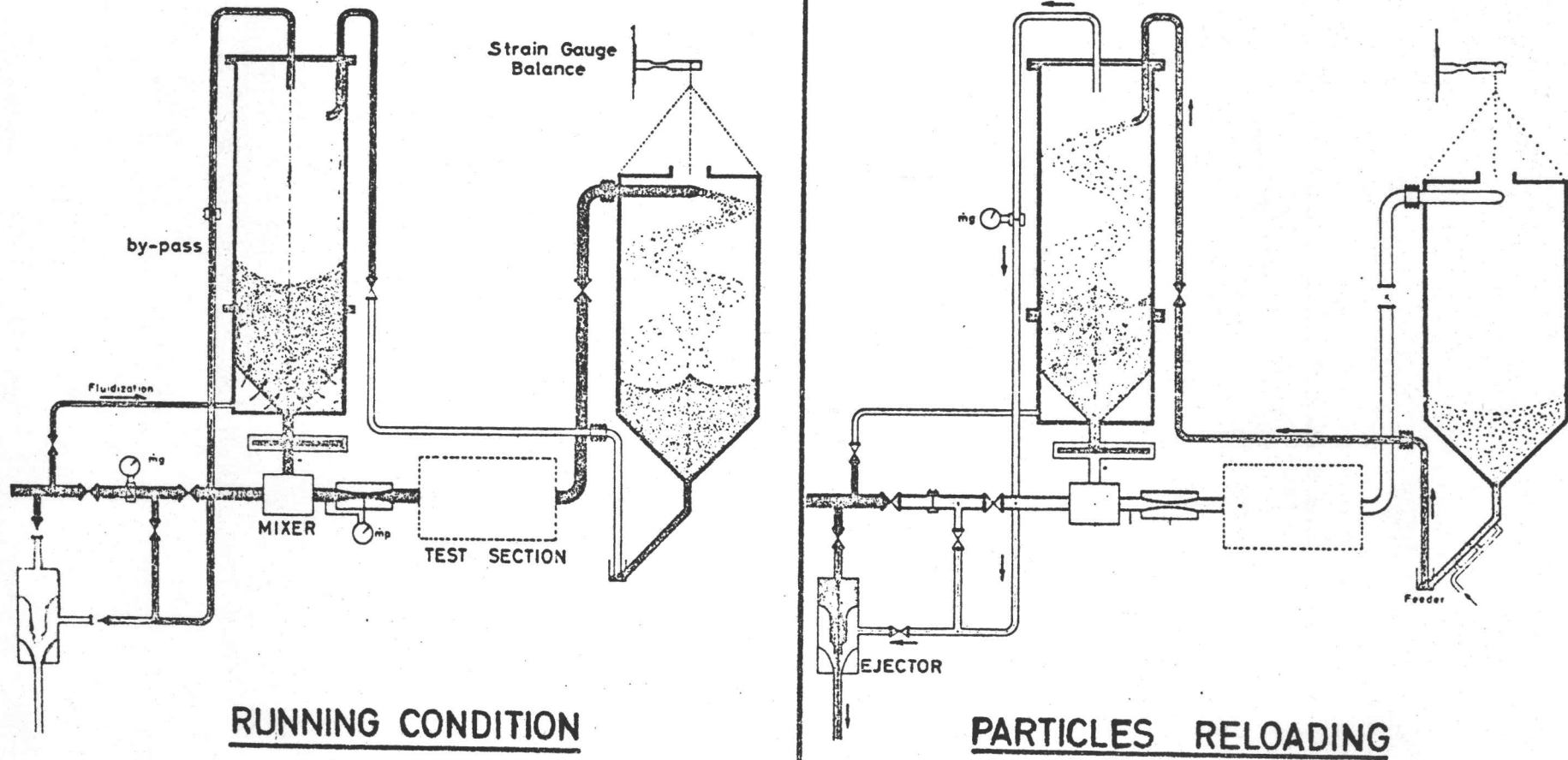
Figure 8



SOLID COLLECTION ANGLES

Figure 9

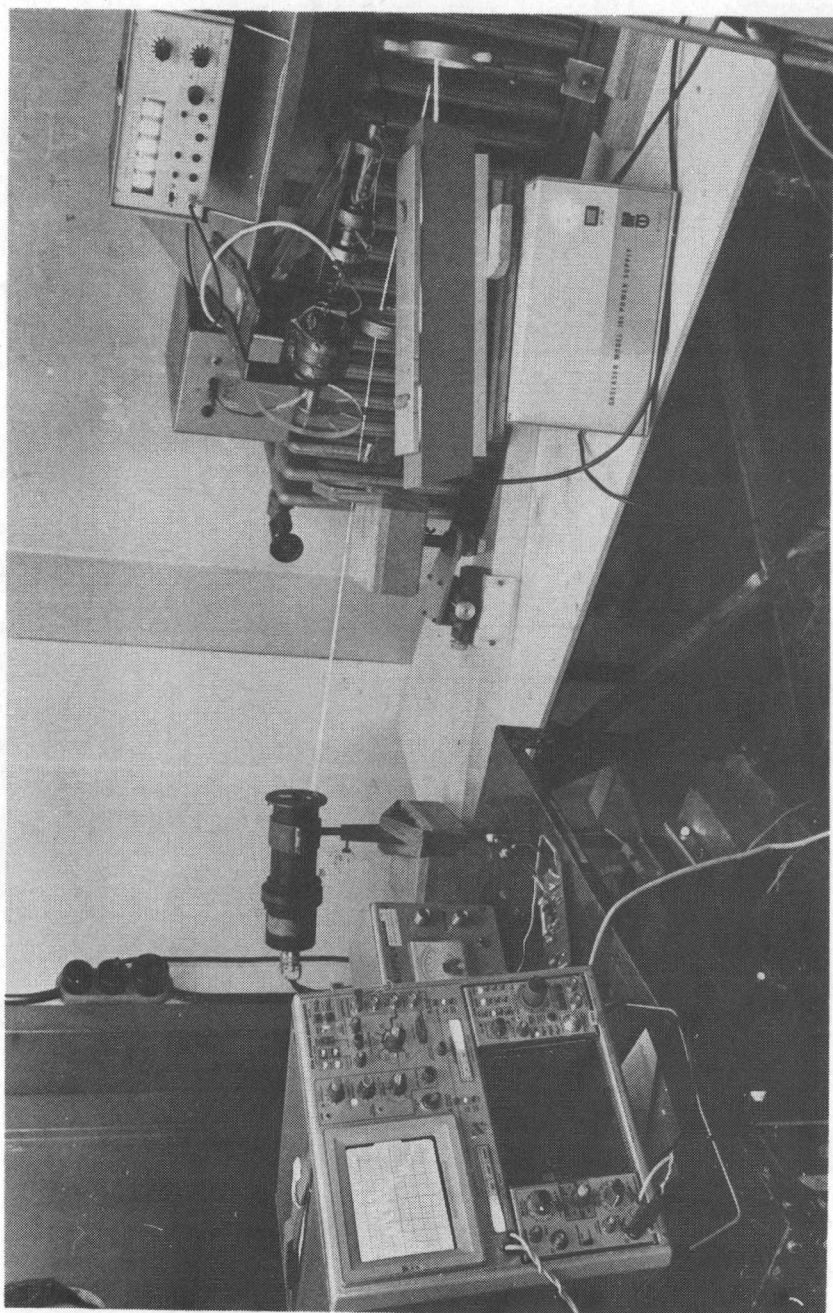
GAS PARTICLES FACILITY - P1-



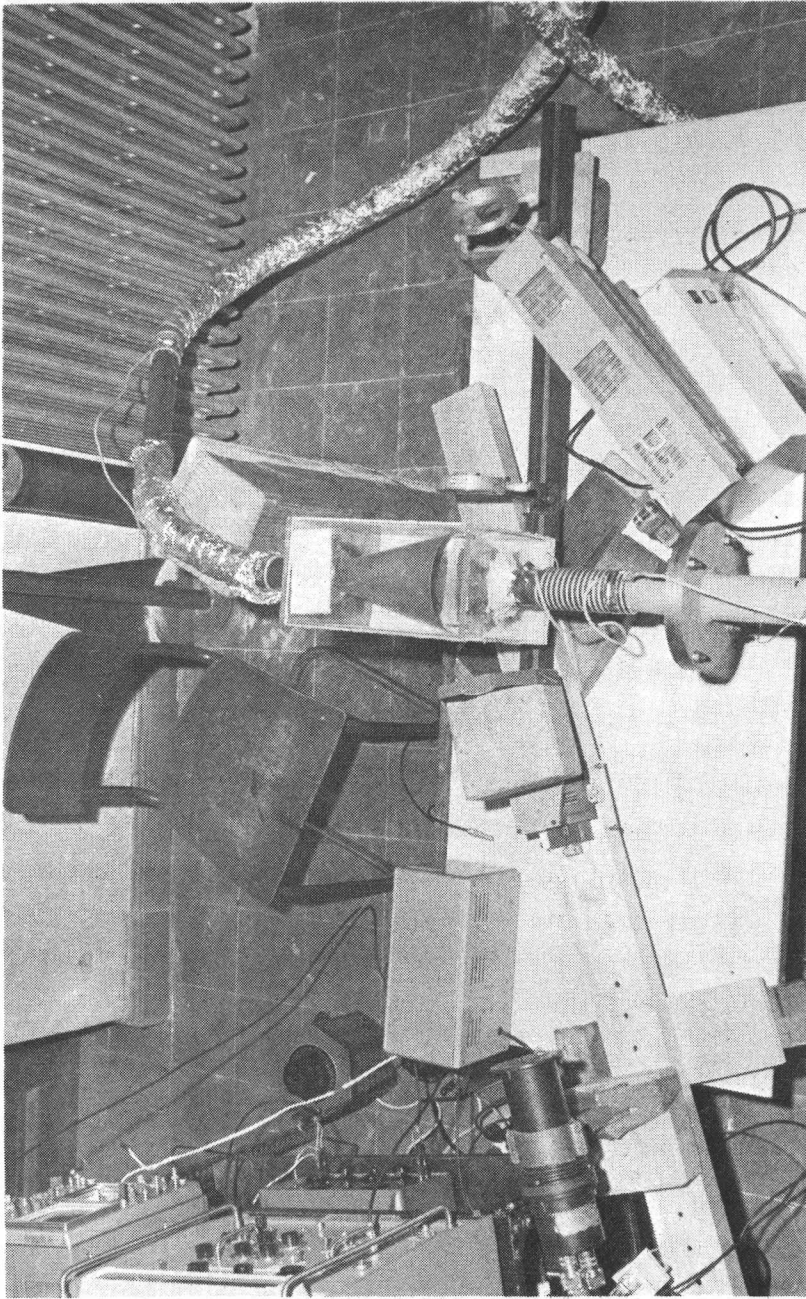
RUNNING CONDITION

PARTICLES RELOADING

Figure 10



Simulation Wheel
Figure 11a LASER DOPPLER TEST SET UP



Flow Facility
LASER DOPPLER TEST SET UP

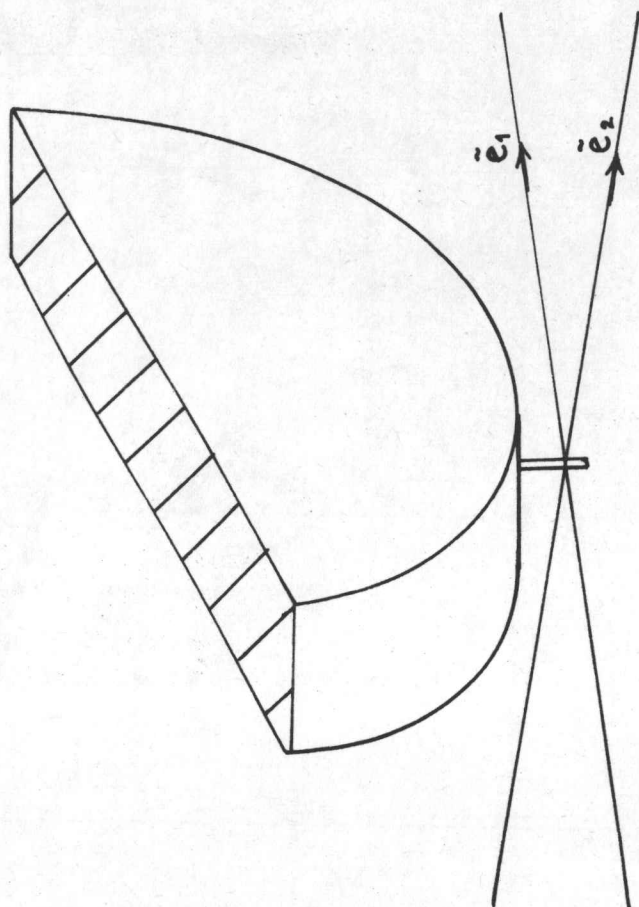
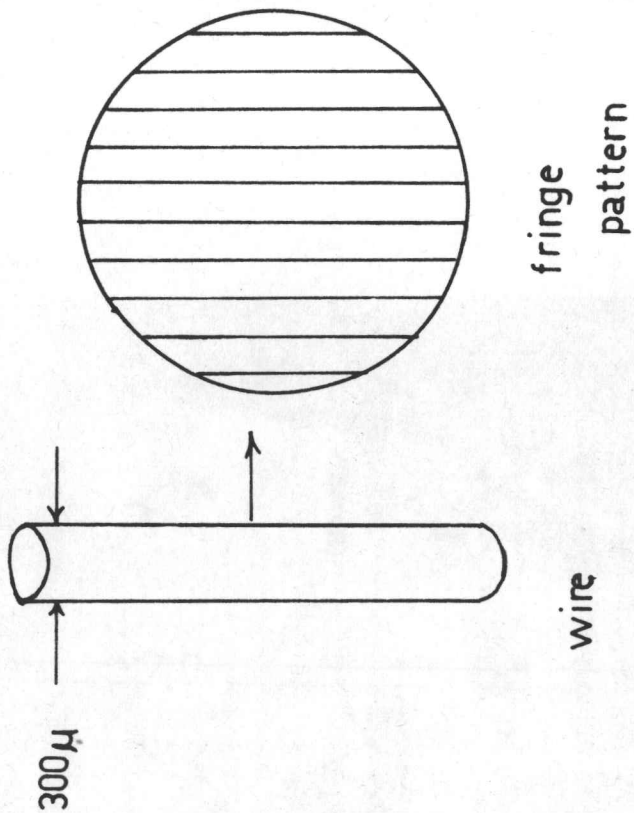
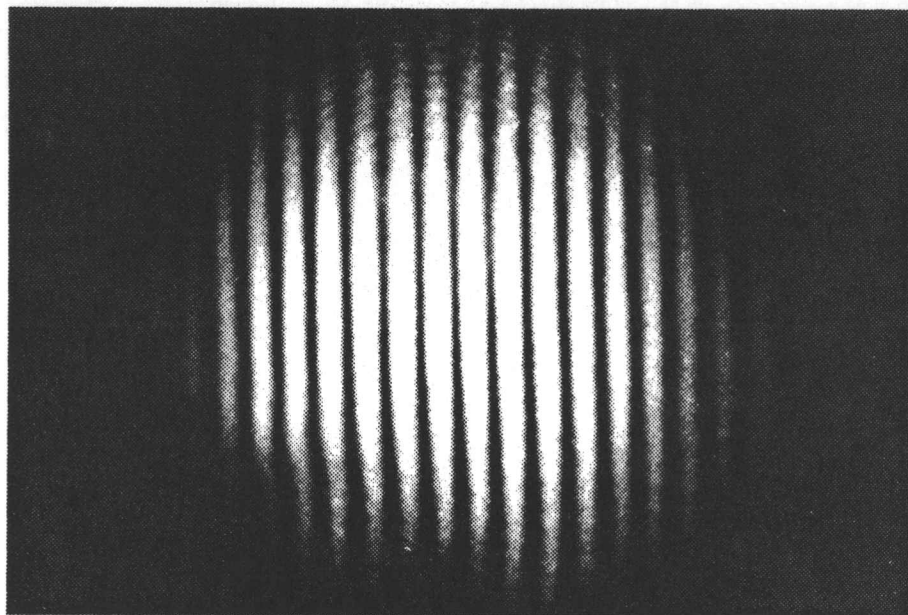


Figure 12

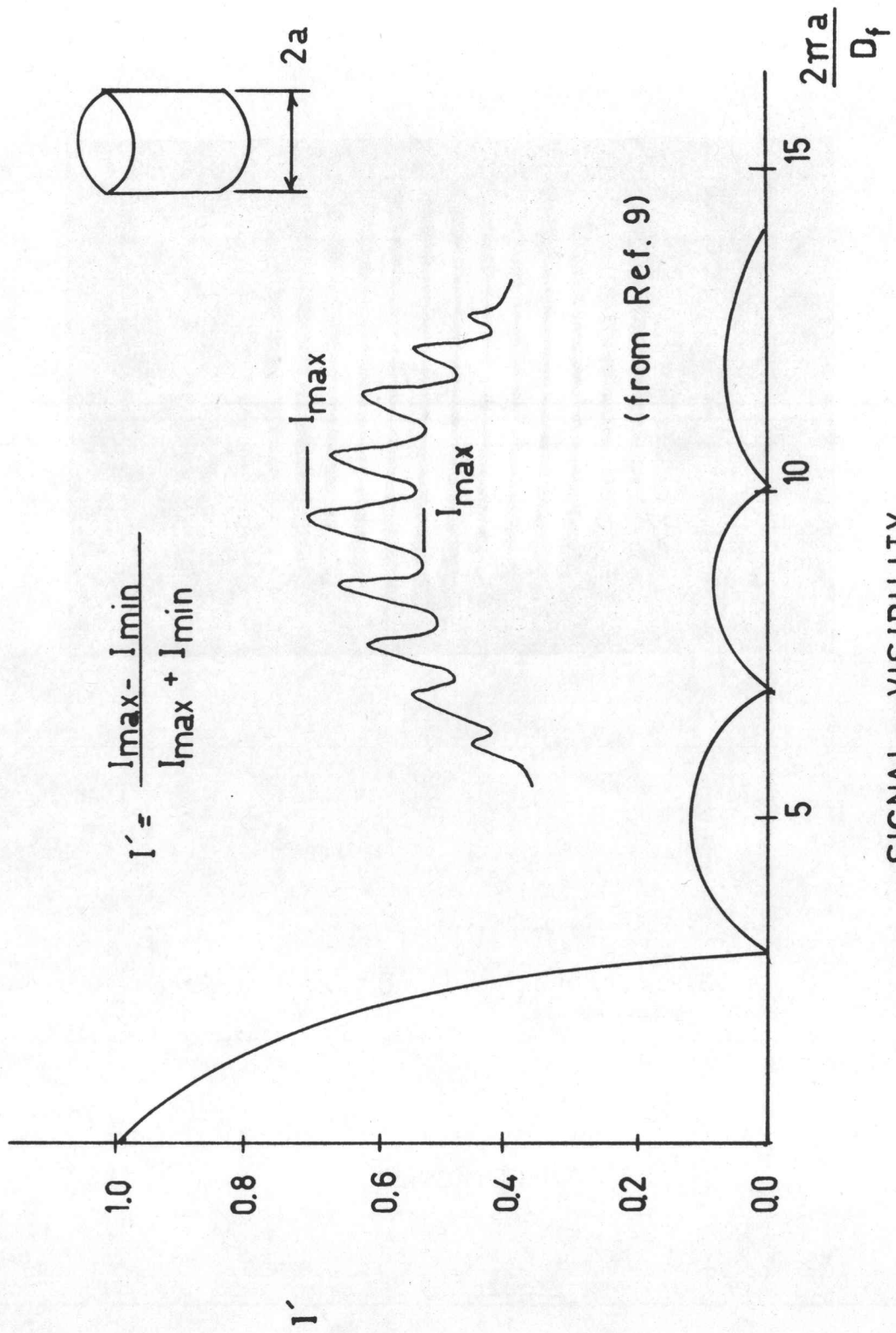


$D_f = 32.2$ microns

$\theta = 2.25$ degrees

FRINGE PATTERN

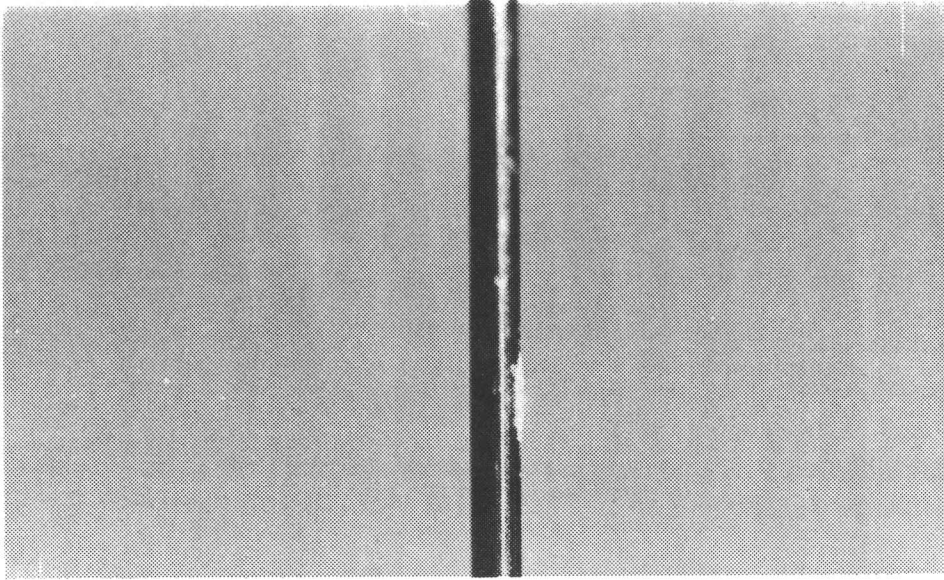
Figure 13



$$I' = \frac{I_{max} - I_{min}}{I_{max} + I_{min}}$$

(from Ref. 9)

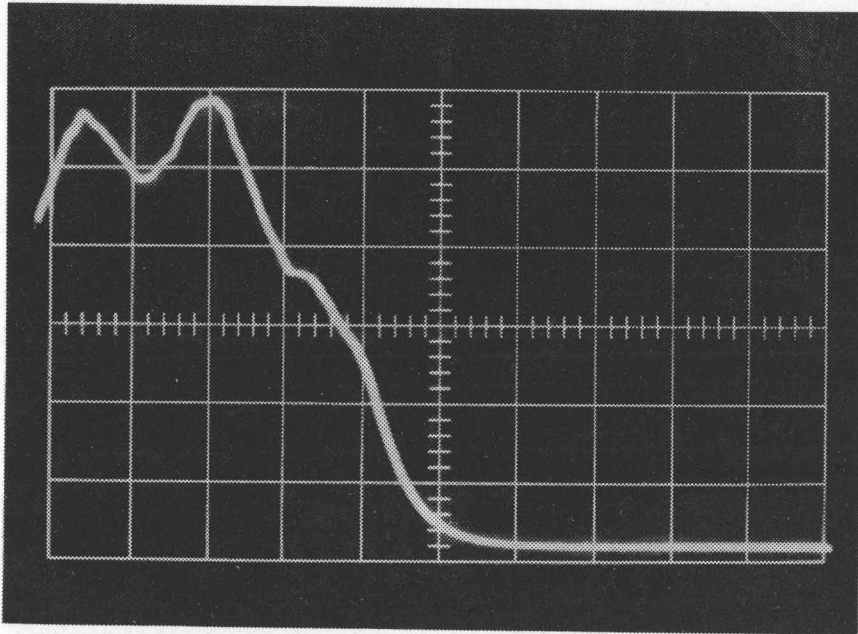
SIGNAL VISIBILITY
Figure 14



Effective particle size observed on 300 micron wire

WIRE REFLECTION

Figure 15

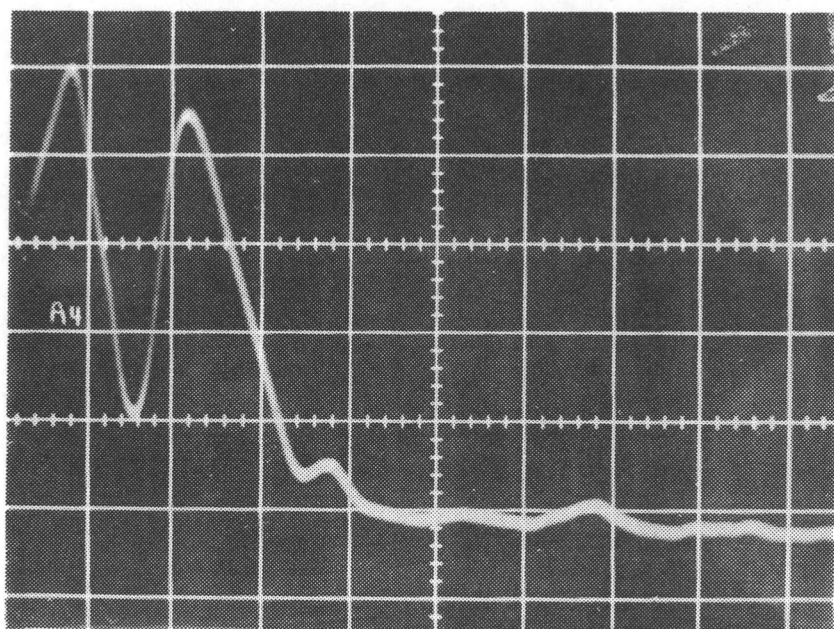


$D_f = 150$ microns

$t = 50$ microseconds / div

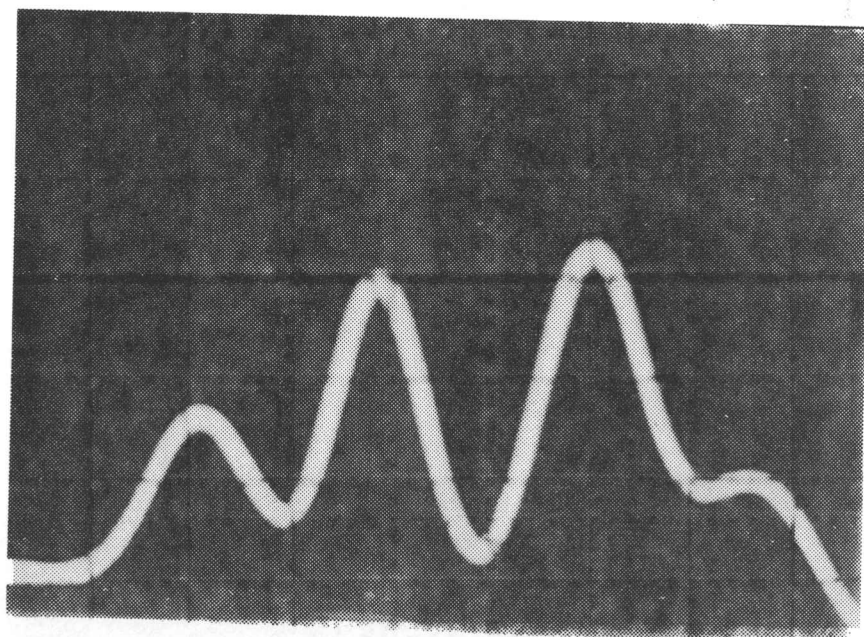
Signal, Particle on Simulation Wheel

Figure 16



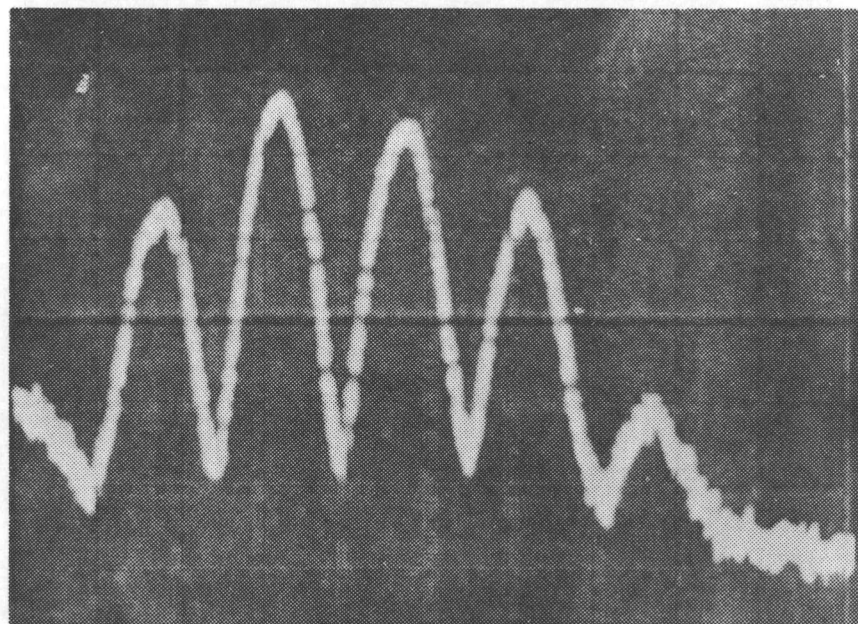
$D_f = 140$ microns $t = 20$ microseconds / div
Signal, Wire on Simulation Wheel

Figure 17



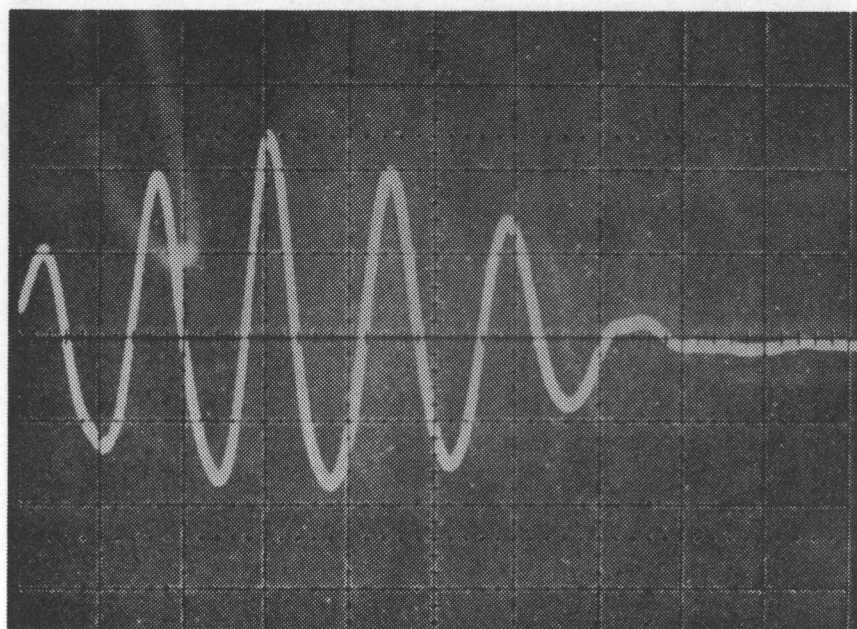
$D_f = 140$ microns $t = 20$ microseconds / div
Signal, 500 micron Particle

Figure 18



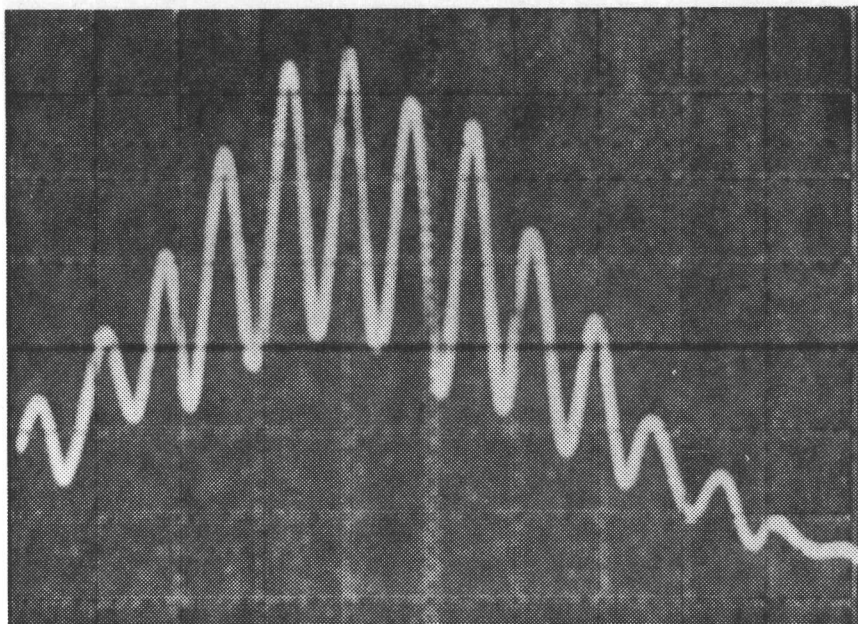
$D_f = 106$ microns $t = 20$ microseconds / div
Signal, Wire on Simulation Wheel, No Filter

Figure 19



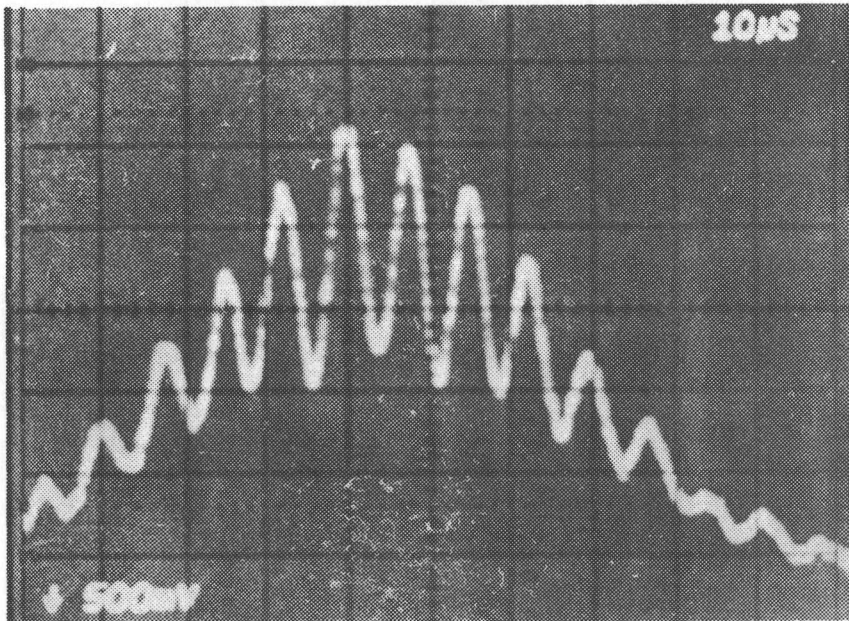
$D_f = 106$ microns $t = 20$ microseconds / div
Signal, Wire on Simulation Wheel, High/Low Pass Filter

Figure 20



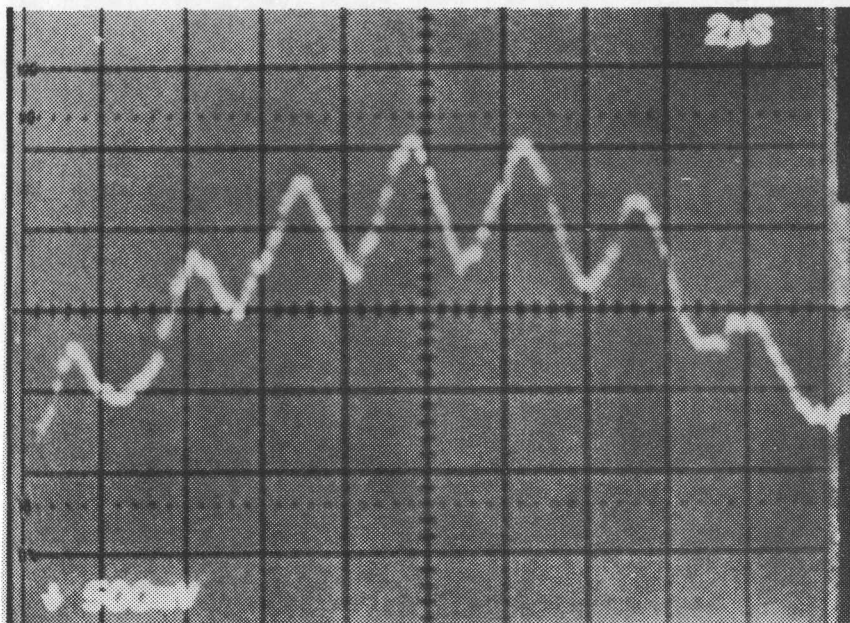
$D_f = 28$ microns $t = 20$ microseconds / div
Signal, Wire on Simulation Wheel, Increased
Number of Fringes, Low Pass Filter

Figure 21



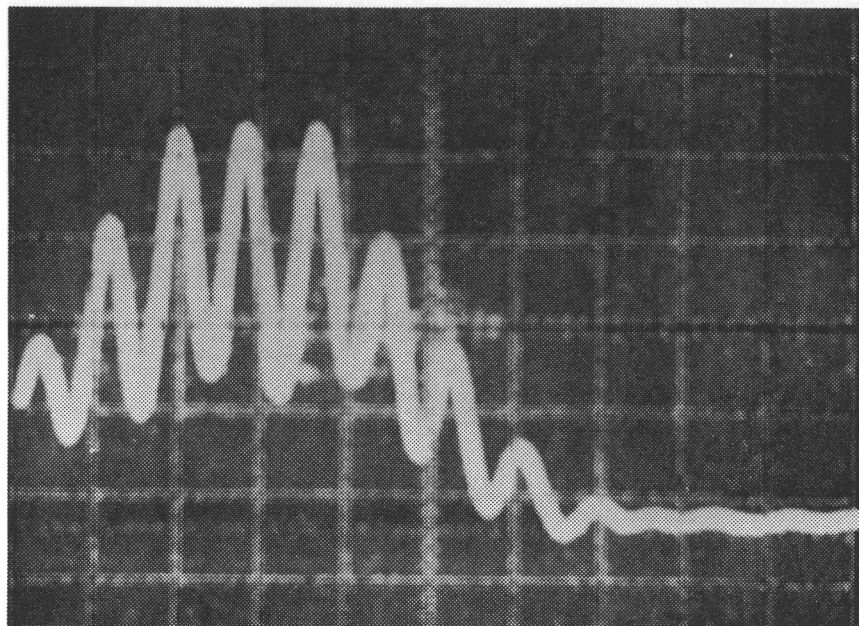
$D_f = 34.2$ microns $t = 10$ microseconds / div
 Signal, Wire on Simulation Wheel, No Filter, $V = 4.78$ m/s

Figure 22



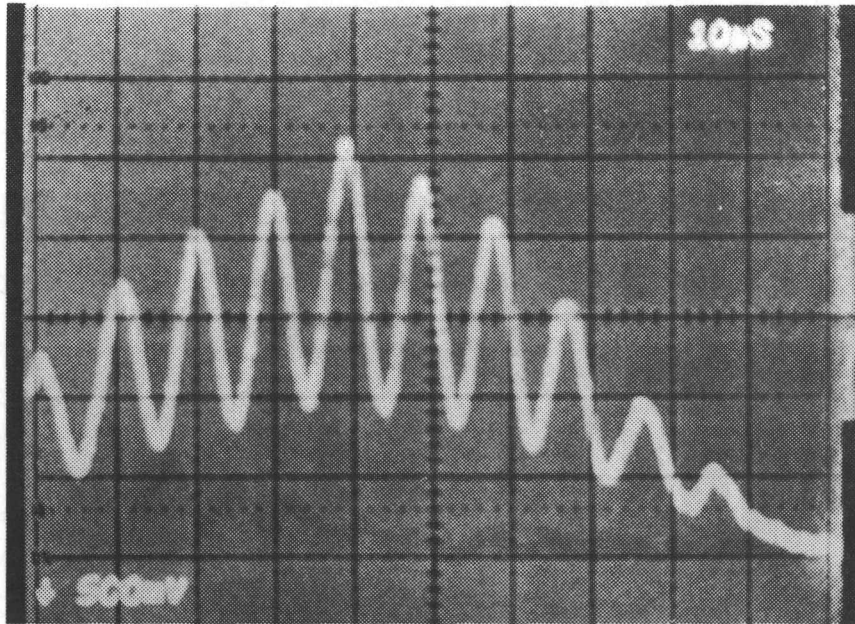
$D_f = 34.2$ microns $t = 2$ microseconds / div
 Signal, Wire on Simulation Wheel, No Filter, $V = 12.35$ m/s

Figure 23



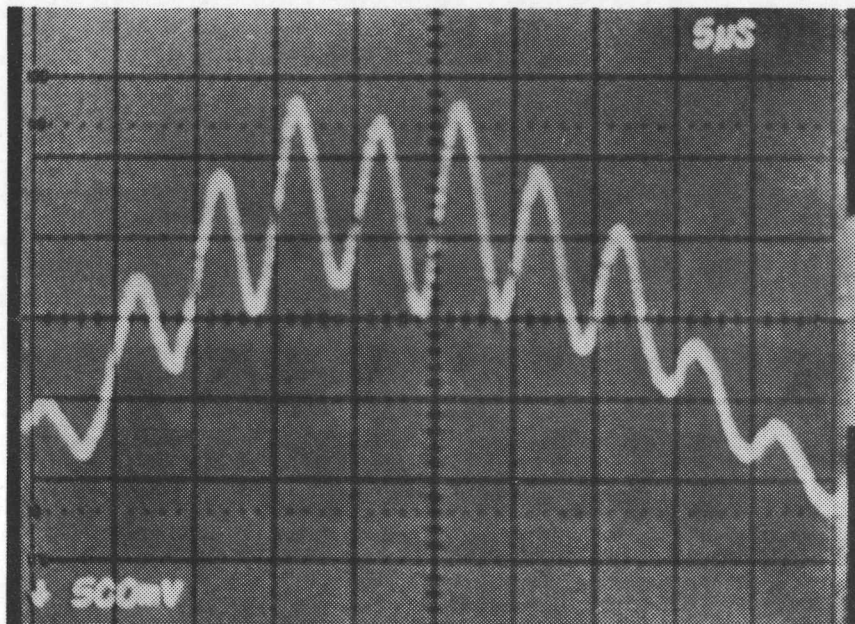
$D_f = 30.4$ microns $t = 10$ microseconds / div
Signal, 100 micron Particle, Low Pass Filter

Figure 24



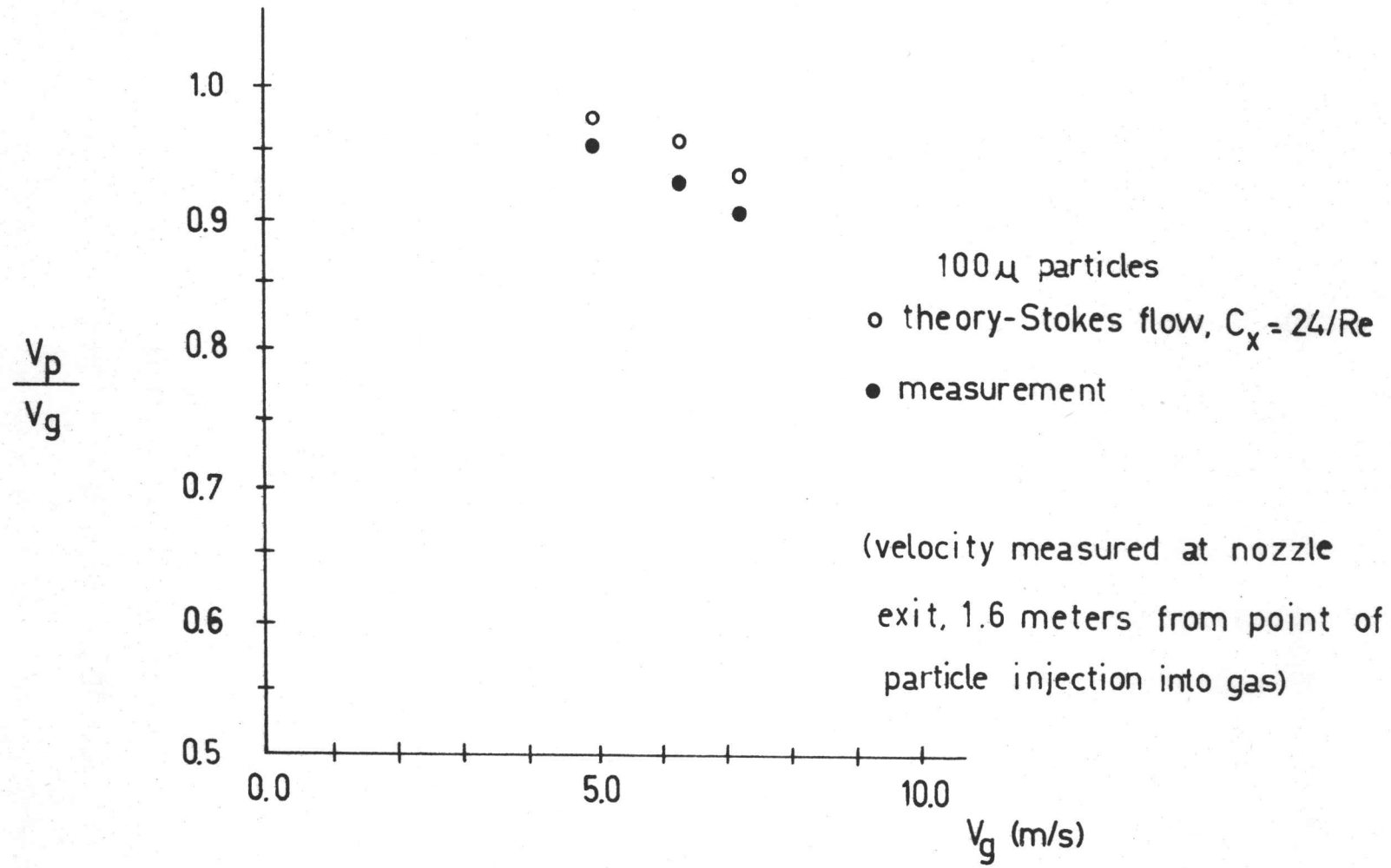
$D_f = 34.6$ microns $t = 10$ microseconds / div
Signal, 500 micron Particle, No Filter, $V = 3.65$ m/s

Figure 25



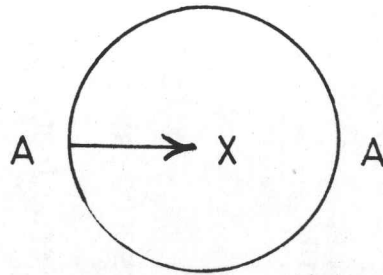
$D_f = 34.6$ microns $t = 5$ microseconds / div
Signal, 500 micron Particle, No Filter, $V = 6.95$ m/s

Figure 26

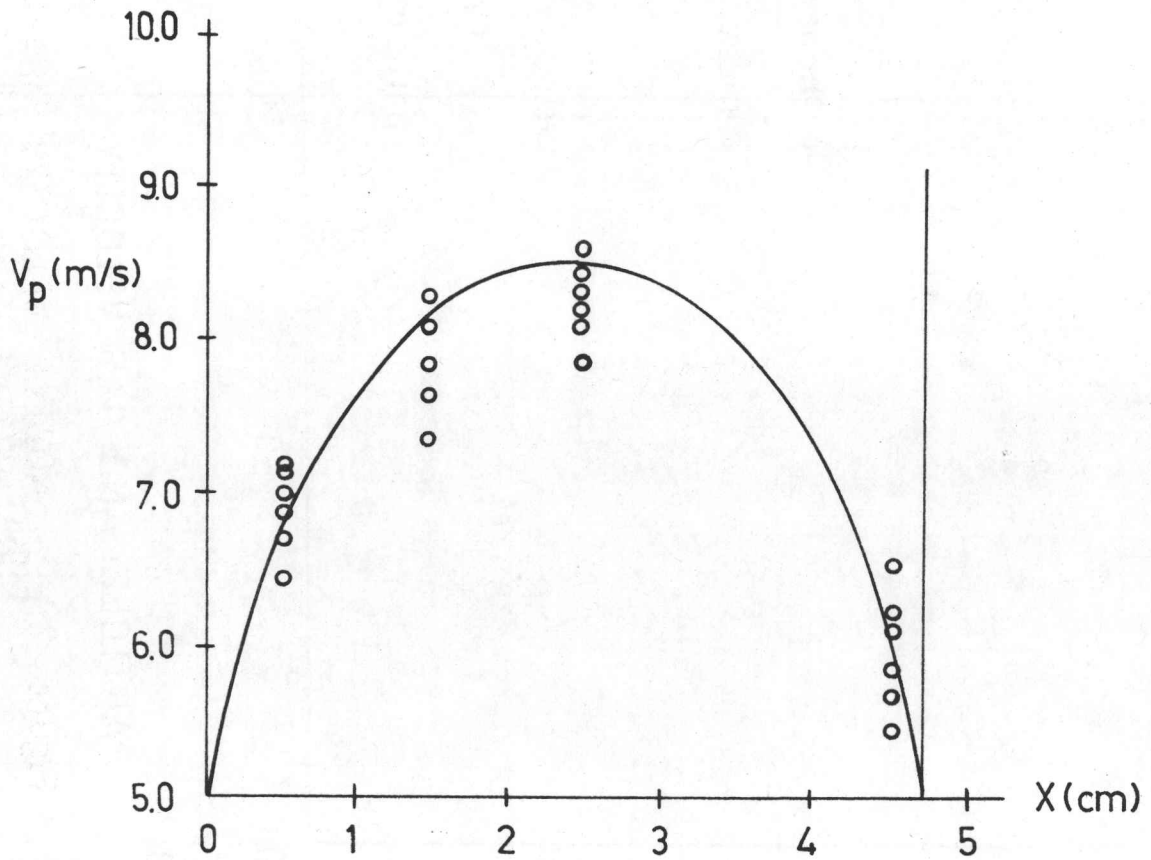


PARTICLE AND GAS VELOCITY

Figure 27



NOZZLE EXIT



o velocity measurements

500 μ particles

NOZZLE VELOCITY DISTRIBUTION

Figure 28

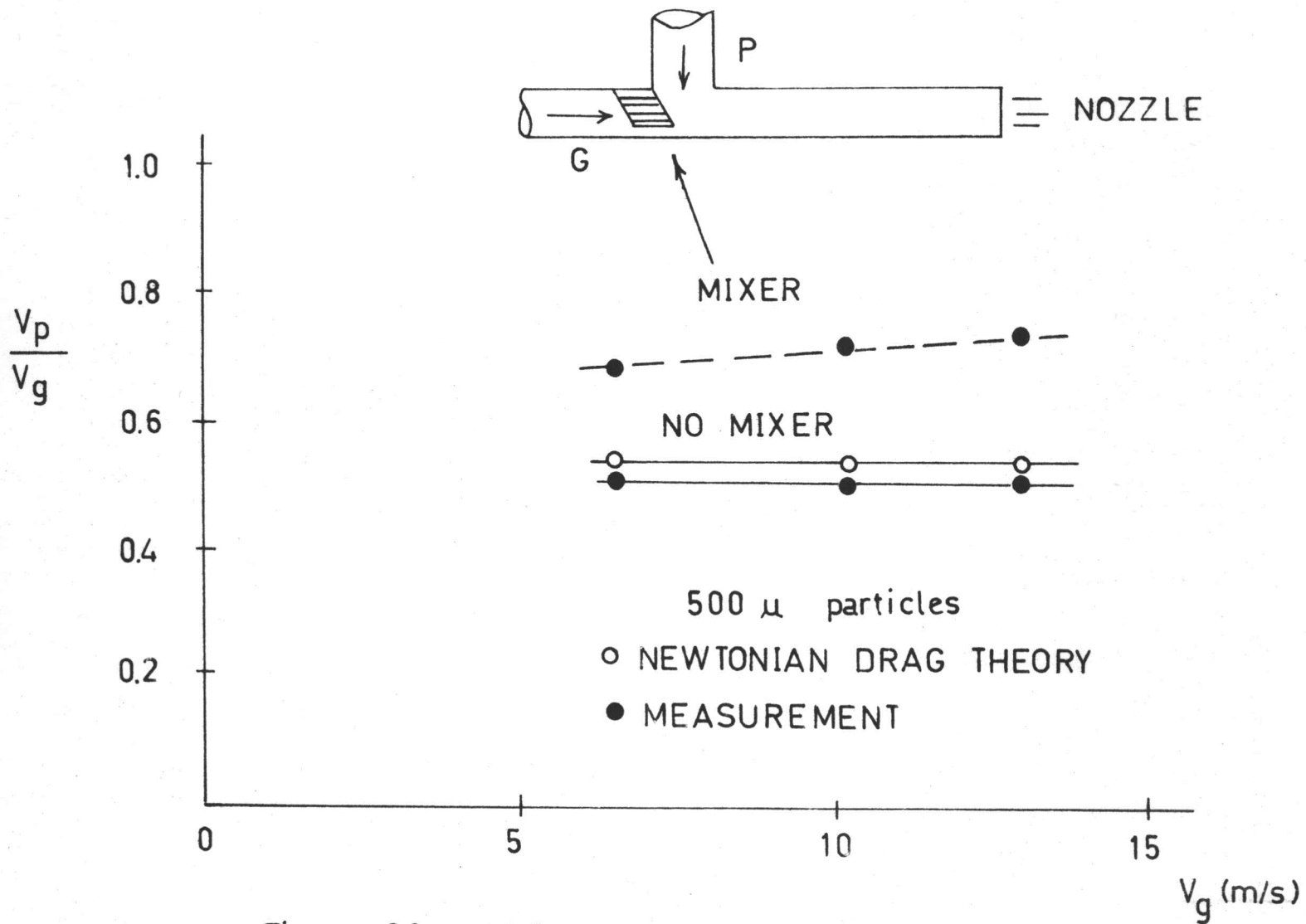


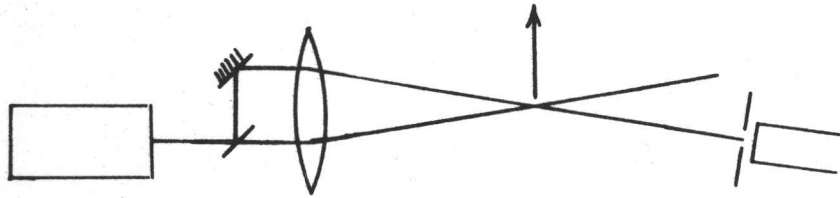
Figure 29 NOZZLE VELOCITY MEASUREMENT

APPENDIX 1

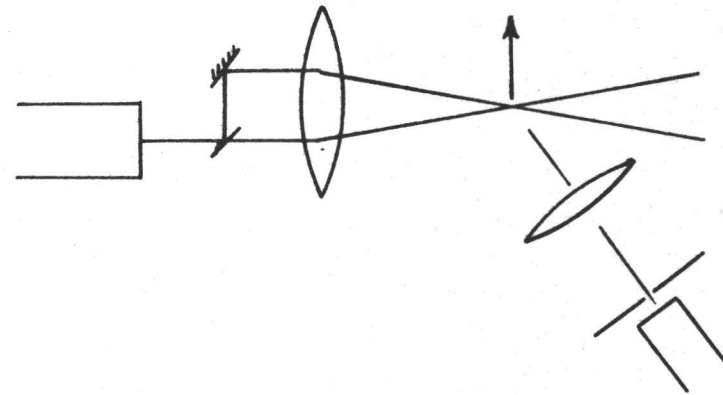
Integrated Optical Unit

In order to eliminate the problems posed by the crude optics currently used for velocity measurements, an integrated unit was designed fashioned after those developed by Durst & Whitelaw (8,10). This unit will provide increased flexibility for variation of the angle between the two laser beams through the use of a movable beam splitter and mirror, and allow the utilization of alternate laser-doppler techniques. Full use of the laser power can be made with any laser-doppler technique shown on the following page, allowing extension of the present velocity range for particle velocity measurements.

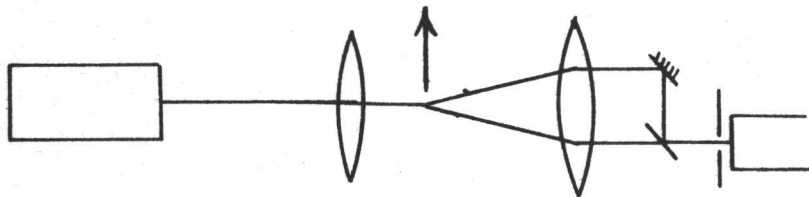
REFERENCE BEAM



FRINGE METHOD



SINGLE BEAM



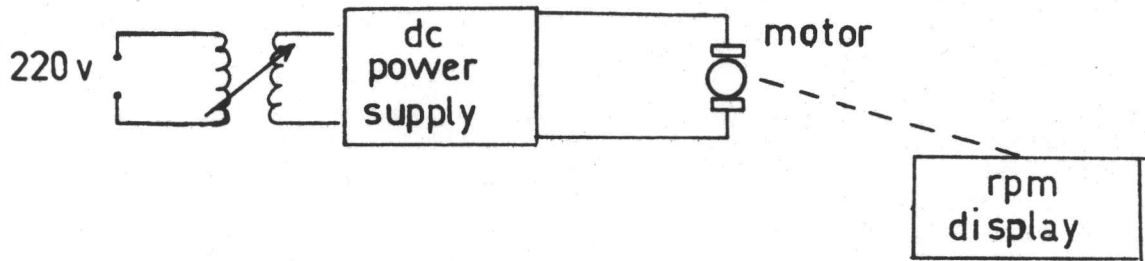
OPTICAL UNIT MODES

APPENDIX 2

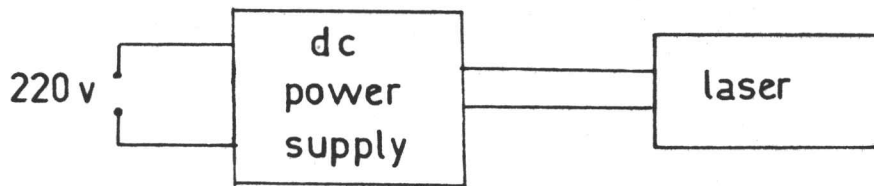
Fringe Laser-Doppler Velocity Meter Equipment

- 1 OIP model 165 He-Ne Laser (1 milliwatt)
- 1.0 meter optical bench and supports
- 1.4 meter optical bench and supports
- Visualization Box
- Reflecting Glass (1.15 & 11.25 mm)
- 1 Converging Lens ($f' = 100$ mm)
- 1 Converging Lens ($f' = 165$ mm)
- 1 EMI model 9558 photomultiplier & emitter follower
- 1 20X microscope lens
- 1 500 KHz filter
- 1 40-430 KHz filter
- 1 0-200 KHz filter
- 3 15 volt power supplies
- 1 2000 volt power supplies
- 1 Voltmeter
- 2 Variable Transformers
- 1 Oscilloscope - Tektronix model 7514
- 1 Electronic Counter - Hewlett Packard model 524C

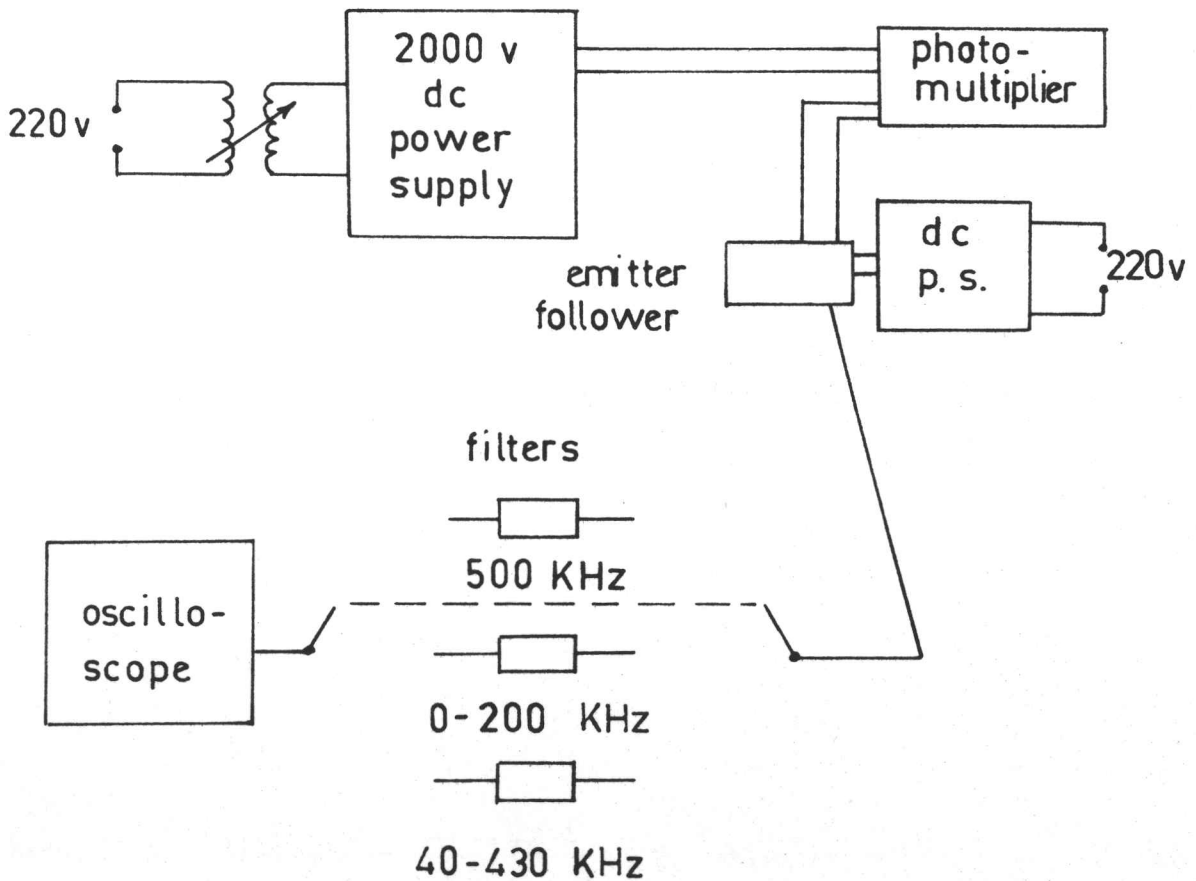
SIMULATION WHEEL



LASER



RECEIVING & DISPLAY EQUIPMENT



LASER DOPPLER CIRCUITS